Chapter 9

# Goal- and Object-Oriented Models of the Aerodynamic Coefficients

Jozsef Rohacs

Additional information is available at the end of the chapter

http://dx.doi.org/10.5772/intechopen.71419

**Abstract**

Nowadays, aeronautics discovers new ways of flights near the critical regimes, unconventional aircraft forms, utilizing the micro–electro-mechanical technologies in flow and aircraft control, adaptive and morphing structures, using the structures and controls based on the biological principles, developing highly flexible structures, etc. Before deployment, these new technologies and solutions must be evaluated, tested in wide aerodynamic, flight dynamic simulations that require improved and new type of aerodynamic coefficient models. The chapter overviews the applicable models of the aerodynamic coefficients, introduces some new models and demonstrates how the different models can be applied in different goal- and object-oriented solutions. The following will be shortly explained: (i) how the aerodynamic forces and moments are generating, (ii) how the linear, nonlinear, steady, and nonsteady aerodynamic coefficient structures and forms might be modeled, and (iii) how to harmonize the model with the goal and object of investigations.

**Keywords:** aerodynamic coefficients, models of aerodynamic coefficients, critical regimes

## 1. Introduction

Aerodynamics is a fundamental subject investigating the interaction of the (atmospheric) gases with objects moving in them. This is a basic science that explains how to develop flying objects (aircraft) with minimum drag, maximum lift, and acceptable and controllable side force and moments.

Aerodynamics [1–8] deals with the theory of aerodynamic force and moment generation and the description of force and moment components appearing on aerofoils, wings, rotating wings, circular bodies at low, moderate, subsonic, supersonic, and hypersonic speeds and

developing the models and methods of calculating the aerodynamic forces and moments. The theoretical and practical methods of evaluation and estimation of the aerodynamic forces and moments are synthetized in aircraft aerodynamic design, i.e., finding the best aerodynamic shape of the aircraft with maximum lift and minimum drag (ratio of which is called as aerodynamic goodness) and controllable other force moments. The aerodynamic characteristics are applied in aircraft motion description, namely for estimating the flight performance, determining the stability conditions and stability, flight dynamics and control.

Aerodynamics is a subfield of fluid and gas dynamics and uses their basic equations. However, there are no good and general methods for calculating the aerodynamic forces and moments that depend on shape and geometrical characteristics of the body, fluid properties, and motion dynamics. Therefore, a series of nondimensional aerodynamic coefficients were introduced, and with the use of results from theoretical and practical investigations (including the computation fluid dynamics and wind tunnel and flight tests), different models of aerodynamic coefficients were developed. The models depend on the real situations, objects, and goals of their application as shown in **Figure 1**, reflecting the aerodynamic mathematical modeling approach of Tobak [11] in the form of known Bisplinghoff's representation [12].

This chapter describes the goal- and object-oriented models of the aerodynamic coefficients and discusses their applicability. It contains 10 subchapters (10 points). The first is this introduction. The second one shortly explains the aerodynamic force and moment generation. The third point introduces the aerodynamic coefficients and defines their mathematical models. The fourth subchapter deals with the first, simple models based on several partial derivatives. The fifth point states improvement of the simple models and describes the so-called classic aerodynamic models. Generally, these models are most used by aerodynamics, flight performance, stability, flight dynamics, and control. The developed aerodynamic models described

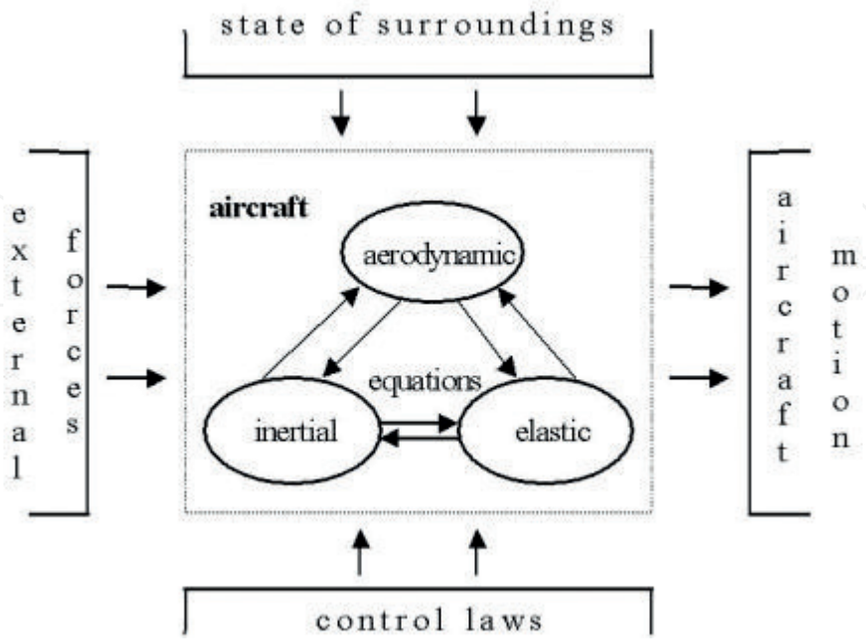


**Figure 1.** Modeling approach to aerodynamic coefficients (affecting aspects) [9, 10].

http://dx.doi.org/10.5772/intechopen.71419

by the next point are used for nonsteady aerodynamics, studying the very nonlinear and even chaotic motion of aircraft. The seventh point shows how the advanced aerodynamic coefficient might be created including the analytical models, special approximation of the measured data, using the soft computing to estimate the coefficient models. Applicability of the described models is discussed in the following eighth subchapter. Finally, the ninth point shows a use of an advanced aerodynamic model. The conclusion (tenth point) summarizes the materials introduced and described by this chapter.

## 2. Aerodynamic force and moment generation

Aerodynamic force and moment are represented and investigated by their components due to the applied reference (coordinate) system. There are several reference systems used. When investigating the stability and control [13–15], the usual body reference is applied, where the center of a right hand Descartes system is located at the aircraft center of gravity and the $x0z$ plane in symmetry plan of body. This system is often used as an inertial reference system, because it is rather close to the inertial system (when the main axes are the inertial axes of the body). The wind reference system is used for studying the flight mechanics and flight performance. This system is derived from the body system by directing the x axis to the aircraft real motion velocity (**Figure 2a**). (The $x0z$ plane is still in aircraft symmetry plan.) **Figure 2b** applies the body axis to aerofoil (wing section) 2D case.

The first explanation of the lift generation can be derived using complex potential flow. Applying the double source and uniform flow for modeling the fixed cylinder moving in ideal (viscosity less) flow, the results show that no lift and no drag are generated on the body, and the velocity/pressure/distribution on the cylinder is symmetric (**Figure 3a**). By including the potential vortex into the model being described, the rotated cylinder in the ideal flow, the results lead to fundamental theorem, called Kutta-Joukowski theorem explaining that the lift is generated because the vortex appears around the body (**Figure 3b**). In ideal flow, there is no drag (flow in **Figure 3b** is symmetric to vertical axis).

Kutta-Joukowski theorem [6]: $L = \rho V \Gamma$, where $L$ is the lift; $\rho$ and $V$ are air density and velocity; and $\Gamma$ is the vorticity, which means lift can be generated only in cases when a vortex appears around the body.

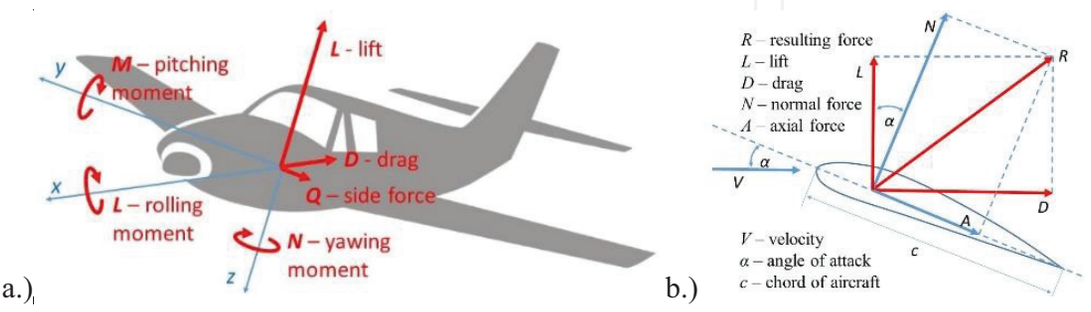


**Figure 2.** The components of the aerodynamic force and moments generated on the aircraft (a) and airfoil (b).

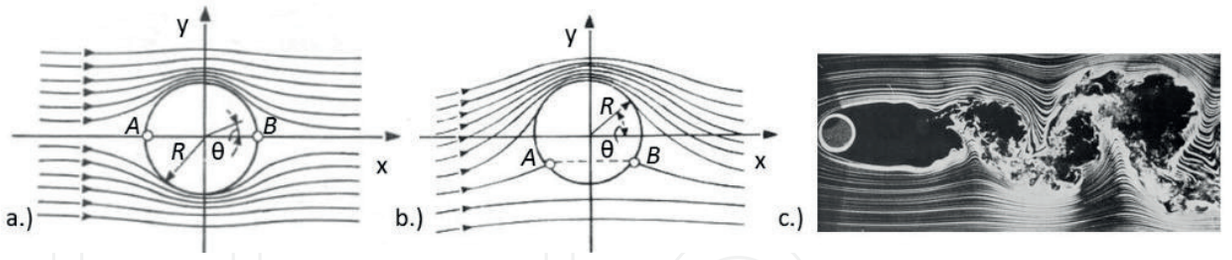


**Figure 3.** The flow around the fixed (a) and rotated (b) cylinders in ideal flow and flow separation from cylinder moving real flow [16] (c) (*R* is the radius of the cylinders [17]; *A* and *B* are the stagnation points in which the flow velocity equals to zero).

In real flow, because the viscosity, drag is generated too (D'Alambert paradoxon), due to flow separation (**Figure 3c**). Prandtl introduced an excellent idea [18]: flow near the body surface must be described as real flow, and flow outside this layer, called boundary layer, can be represented as ideal flow. In the boundary layer, the flow might be laminar, when the sublayers near the body surface move parallel, but with different velocities, or turbulence, when the flow particles move in a chaotic ways [1, 5, 6]. The developed boundary layer theories [19, 20] may well define the skin friction drag, drag appearing in boundary layer (**Figure 4a**).

On the other hand, the drag has several components [1–8] (**Figure 4b**). The induced drag is affected by the vortex lines separating at the wing tips. There is no lift without vortex, while vortex induces some drag.

The drag resulting from pressure distribution on the body surface and skin friction drag together is called as profile drag. Flow separation drag is the drag initiated by separation of flow (at high speed or at high angle of attack). Wave drag is caused by the shock wave system appearing at high subsonic, transonic, and supersonic speeds. The interference drag is the extra drag affected by interaction of the flows around the different elements of aircraft (or even different aircrafts). The 3D drag is an interesting special drag component caused by effects of 3D aspects. Finally, the aircraft components like radio antenna add the aircraft components' drag. Often, especially for subsonic cruise speed, the drag is classified by the use of so-called causal breakdown, and when the pressure and friction drag are composed from flat plate friction, drag components are affected by protuberances, roughness, and incremental profiles.

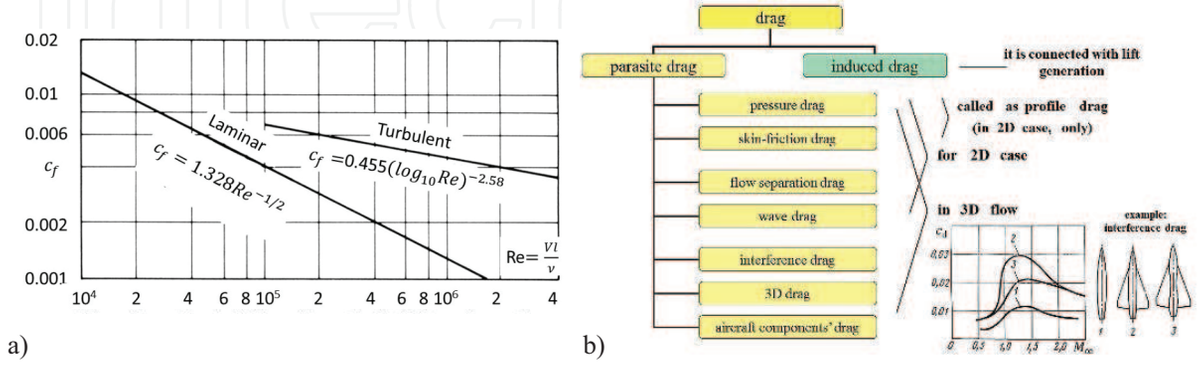


**Figure 4.** Skin friction drag of the thin plate (a) depending on the Reynolds number (Re = flow velocity × length/air kinematic viscosity) and classification of the drag (b).

http://dx.doi.org/10.5772/intechopen.71419

Mathematical investigation and calculation of the aerodynamic forces and moments are supported by computational fluid dynamics (CFD) [21–23]. Nowadays, several well-applicable software are available. The cost- and time-effective CFD technology allows to simulate and compute (i) all the desired quantities (stream functions and vorticity, including the integral quantities as lift, drag, and moments), (ii) with high resolution in space and time and it is applicable to (iii) actual flow domain, (iv) virtual problems, and (v) realistic operating conditions, as well as (vi) excellent visualization and (vii) systematic data analysis of the results (**Figure 5**). Numerical aerodynamics may give excellent results in simplified cases or after serious adaption (verification and validation) to the investigated situations. Generally, the quality of the CFD results depends on managing the uncertainties (real turbulence and their modeling [26]) and so-called unacknowledged errors (as logical mistake in using the software, errors in parametrization, models of boundary conditions, bugs, etc.).

The practical measurements and estimations of the aerodynamic forces, moments, and their coefficients by use of wind tunnel and flight tests comparing to CFD are very costly and require lot of time (up to several years) [27–29]. The practical methods might be used for study (i) in limited number of quantity, (ii) in limited number of operational points and time instant, (iii) in limited range of problems and operating conditions, and as usual (iv) with use of small-scale models (**Figure 6a**) or specially equipped aircraft.

The practical measurements (including the flow visualization, studying the flow separation, developing the streamlined bodies, too) support the (i) understanding of the flow structure, (ii) measuring and identification of the aerodynamic coefficients, (iii) verification and validation of

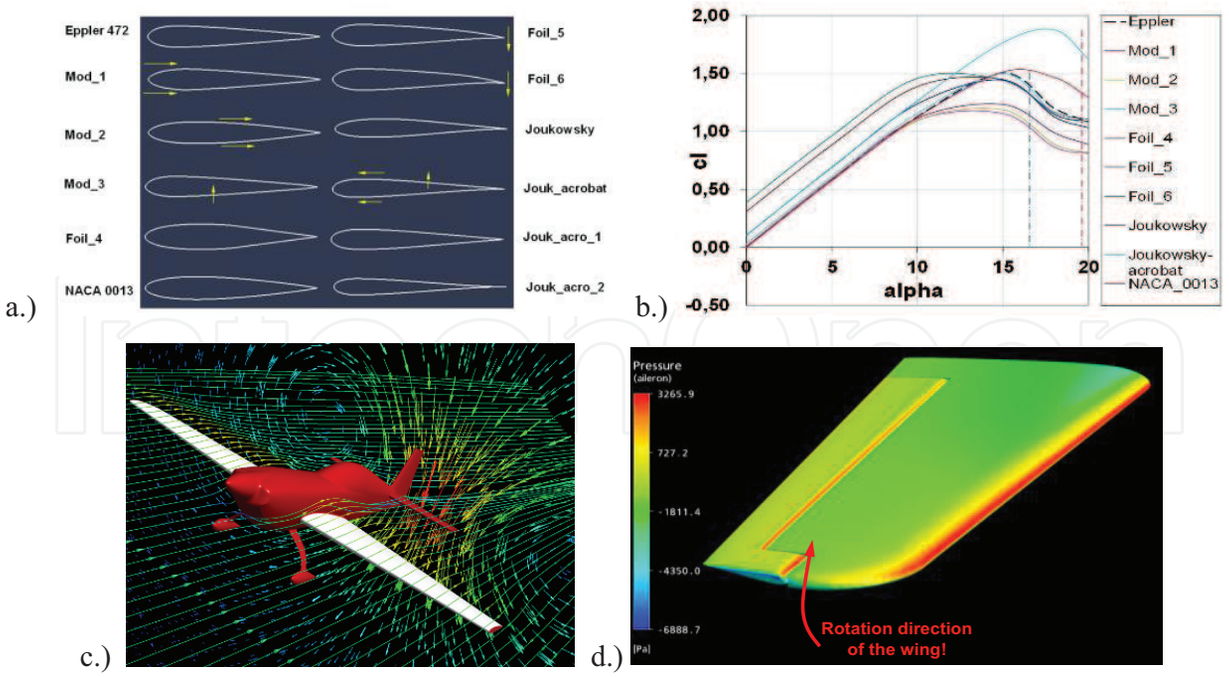


**Figure 5.** The typical example of CFD application to development of a special acrobatic aircraft Corvus Racer 540 [24, 25]. (a) Series of investigated profiles modified from Eppler 472 and Joukowsky, (the yellow arrows show the ways of modification), (b) determined lift coefficient angle of attack curves, (c) the optimized fuselage and the 3D flow with tip vortex, and (d) pressure distribution on wing in high speed rolling.

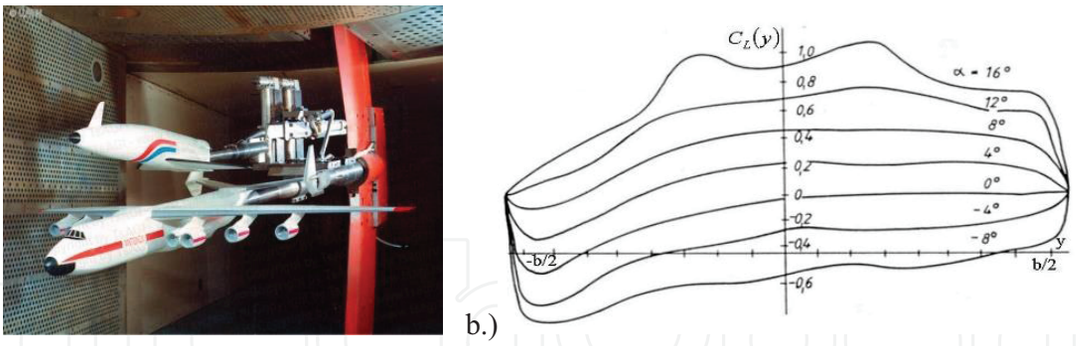


**Figure 6.** The practical measurements: (a) An-225 Mria and space shuttle group model in the wind tunnel at the TsAGI [30], (b) lift coefficient distribution along the wing span (b/2) of deformed (left side) and nondeformed (right hand) wing [31].

the CFD methods, (iv) optimizing shape for cruise flight mode, and (v) studying the most dangerous flight mode, aircraft approach and landing.

**Figure 6b** shows how the real lift distribution depends on the flight conditions, namely how the deformation of wing deformed under loads has influence on the actual lift distribution.

Generally, the differences in calculated and measured wind tunnel lift coefficient reach 7–8%, while, for example, the differences between the measured wind tunnel and flight test drag coefficient equal to 5–10% and up to 18% at the transition period from subsonic to supersonic flights [32]. During the periodic angle of attack oscillation of the wing, there is a large hysteresis in the lift coefficient—angle of attack function. So, there are considerable differences in steady and unsteady regime.

These thoughts on aerodynamic force and moment generation demonstrate that the theoretical calculation and the practical measurements cannot independently provide full and correct description for aerodynamic forces and moments. At first, the semiempirical methods were developed and applied for aircraft aerodynamic design and calculation of the aerodynamic characteristics [33–37]. Later, with gaining in prestige of CFD, the role of modeling of aerodynamic coefficient increased.

## 3. Aerodynamic coefficients

The motion of aircraft can be described by a system of equations describing the motion of center of gravity of aircraft and its rotation around it [13–15]. The general form of the system contains stochastic, partial nonlinear differential equations with delays.

So, this motion can be defined by solving the inertial equations that should be coupled with the equations describing the aerodynamic (gas dynamic) and elastic phenomena (see central part of **Figure 1**) [9, 11, 12]. The latter equations are coupled through the aircraft shape and structure. The time-dependent aerodynamic equations describe the instantaneous aerodynamic effects on the aircraft assumed in the form of aerodynamic forces and moments

http://dx.doi.org/10.5772/intechopen.71419

depending on the state of the flow field surrounding the aircraft, the motion variables, the aircraft shape deformation, and the initial conditions.

In the first approximation, the instantaneous aerodynamic force depends on air density, $\rho$, and velocity, $V$, and mean geometrical parameter of the body, namely wing span, $s$. That by use of methods of dimensional analysis can be represented in the form:

$$F = C\rho^{\alpha}V^{\beta}S^{\gamma}, \tag{1}$$

where $C$ is the coefficient. The exponents $\alpha$, $\beta$, and $\gamma$ must be derived from the condition that the dimension of the different sides of equation should be equal. Using the results $\alpha = 1$, $\beta = 2$, and $\gamma = 2$, the aerodynamic force can be calculated as:

$$F = C\rho^{1}V^{2}S^{2} = 2CAR\frac{\rho V^2}{2}\frac{S^2}{AR} = C_F\frac{\rho V^2}{2}S, \tag{2}$$

where $c_F$ is the so-called nondimensional force coefficient, $AR$ is the aspect ratio ($AR = s^2/S$), and $S$ is the wing area. From here, the aerodynamic force and moment coefficients are:

$$C_F = \frac{F}{\frac{\rho V^2}{2}S}, \qquad C_M = \frac{M}{\frac{\rho V^2}{2}Sc_a}. \tag{3}$$

Here $C_a$ is the aerodynamic chord.

The aerodynamic forces and moments, as well as their aerodynamic coefficients, can be represented by their components:

$$C_F = \left[C_x(=C_D), C_y, C_z(=C_L)\right]^T, \qquad C_M = \left[C_l, C_m, C_n\right]^T, \tag{4}$$

according to the axes of the applied reference system (here wind system) [1, 14].

The nondimensional aerodynamic coefficients fully describe the aircraft aerodynamics [1–8]. The basic aerodynamic characteristics of airfoils [38, 39] are shown in **Figure 7**. The left first figure shows the typical changes in lift coefficient with increase in angle of attack that begins with linear function, followed by nonlinear form at high angle of attack and dropping after separating the flow from the upper surface of aerofoil at the so-called critical angle of attack.

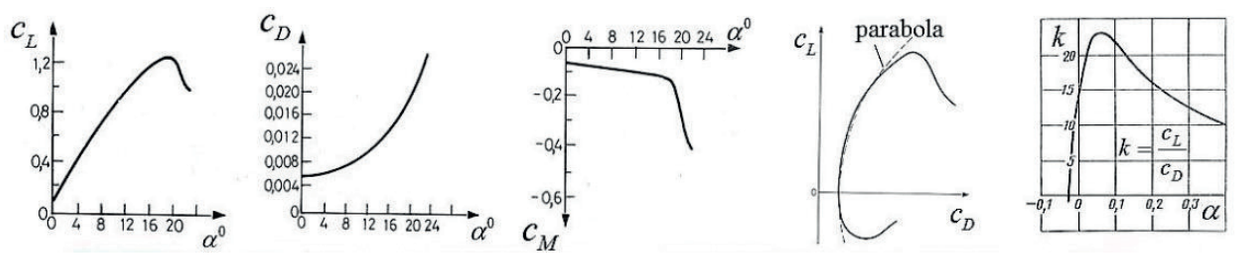


**Figure 7.** Aerodynamic characteristics of an airfoil: lift, drag, and moment coefficients as function of angle of attack, polar curve, and "goodness" factor.

This phenomenon is called stall. The drag coefficient increases with growing lift coefficient due to the induced drag. The moment coefficient follows the changes in lift and drag coefficients, especially after stall. The polar curve ($C_L = f(C_D)$) and "goodness" factor ($k = (C_L/C_D = f(\propto))$) explain the relatively low angle of attack and must be realized during the most important flight regime, during the cruise flight for having minimum drag, minimum required thrust, and minimum fuel consumption.

As it is well known, the subsonic and supersonic aerodynamics is principally different. The "classic" airfoils with blunt leading edge cannot be applied, because their drag tends to the infinity nearing to Mach number (velocity related to the sound speed in the same condition) equals to one. At the supersonic speed only, the airfoils (wing and fuselage) with sharp leading edge can be applied (**Figure 8a**).

**Figure 8b** demonstrates how changes in some parameters may radically affect the aerodynamic characteristics. In case of high aspect ratio wing, the vortex generating the lift as a vortex tube along the wing span separates at the wing tips and causes the induced drag. The low aspect ratio delta wing has unique aerodynamic picture. The flow separating from the wing leading edge and the caused by this separated flow vortexes moving back on the top of the wing generate extra lift at high angle of attack, and the stall appears at 45–70°, only.

The aerodynamic coefficients depending on the flight modes and flight maneuvers are managed by use of control surfaces and motion devices as flaps, slots, and generally by all the devices deviating and changing the geometry like undercarriage system, braking parachutes, etc. [1–8]. For example, the flaps at wing trailing edge and slat at the leading edge (making slots between the slat and mean wing) are used for increasing the lift (and drag) allowing to reduce the take-off and landing speeds for making safer flight modes. The flaps increase the lift coefficients ("moving" the lift coefficient and angle of attack curve left and up in **Figure 9a**), while the slats/slots increase the critical angle of attack, (because they do not change the airfoil/wing chamber). In **Figure 9a**, at low lift coefficient region, the effect of a special leading edge flap, called Krueger flap, is shown, too.

The flaps are deflected on the lower angle during take-off than during landing, because they increase the drag, too. **Figure 9b** demonstrates these changes in polar curve diagrams depending on the flap deflection.

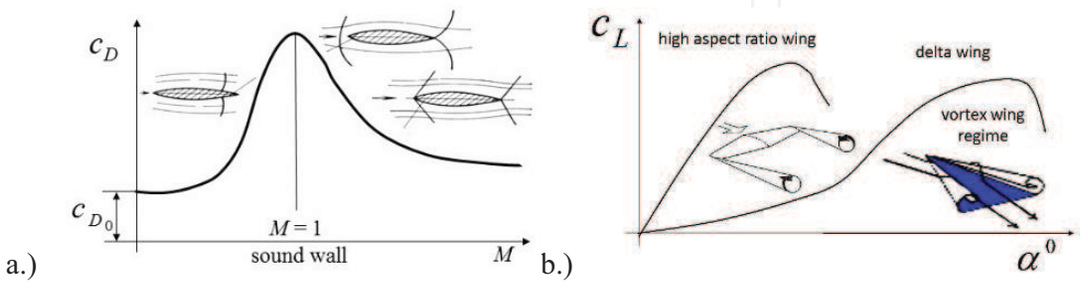


**Figure 8.** Further specific aspects: (a) drag coefficient of the supersonic airfoil depending on the Mach number and (b) lift coefficients generated on the high and low aspect ratio (delta) wings.

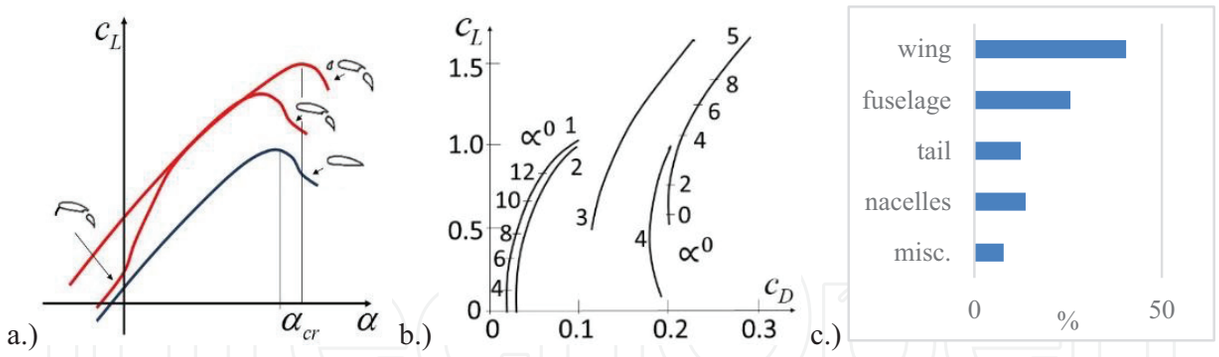


**Figure 9.** An integrated aerodynamic characteristic of the wing (airfoil) and flap/slats (a), polar curve diagrams of a middle size passenger aircraft (b), and drag coefficient breakdown (c). (In figure b, the numbers at curves depict the flight conditions as 1. cruise flight (all devices are closed), 2. undercarriage system is open, only, 3. take-off regime (flaps deflected near $30^0$), 4. landing condition (flaps deflected up to 45°), 5. all the wing mechanisms are opened (slats and interceptors).

**Figure 9c** calls attention to the final aerodynamic coefficients that always are composed from the coefficient generated on/by the aircraft elements.

These examples underline that the aerodynamic characteristics depend on the state of the flow field surrounding the aircraft, like air viscosity, motion variables, e.g., linear and angular velocities, real geometrical characteristics reflecting the effect of the deflection of the control elements and the deformation of aircraft, and they may have a sensitive dependence on the initial conditions (**Figure 1**). Therefore, the aerodynamic coefficients are given in the form of functions of different variables, like position angles and velocities of aircraft, flow characteristics, namely Reynolds number, Mach number (speed), deflection angles of aerodynamic control surfaces, control forces, etc. [1–8]. These functions are very nonlinear and very complicated. In case of dynamic changes in basic parameters (like angle of attack) and especially in case of oscillation motion, the aerodynamic coefficients contain the hysteresis-type nonlinearities depending on the frequencies and amplitudes of oscillation. So, different simplified, more complex, and special models and mathematical representations are needed.

## 4. The first (simple) aerodynamic models

The mathematical descriptions of the aerodynamic coefficients are called as aerodynamic models [1–8]. First models were based on the work of Bryan [40], who used two principal assumptions: the aerodynamic forces and moments depend only on the instantaneous values of the motion variables, and their dependence is of linear character. Therefore, the simple models of the aerodynamic coefficients can be expanded into a Taylor series about the reference states.

$$C_A(t) = C_{A_0} + \sum_{i=1}^{n} C_{a_{p_i}} p_i(t), \tag{5}$$

where $C_A$ is the aerodynamic coefficient, $p_i$, $i = 1, 2, \ldots, n$ are the parameters, $C_{A_0}$ is the aerodynamic coefficient at $p_i = 0, \forall i$ and the $C_{a_{p_i}}$ is the partial derivative coefficient.

$$C_{A_{p_i}} = \left(\partial C_A / \partial p_i\right)_{p_i=0}. \tag{6}$$

For example, the pitching moment in simplified case can be represented by the following term:

$$C_m(t) = C_{m_0} + C_{m_V} V(t) + C_{m_q} q(t) \tag{7}$$

where the $C_{m_V}$ and $C_{m_q}$ are the moment coefficient derivatives:

$$C_{m_V} = (\partial C_m / \partial V)_{V=0}, \qquad C_{m_q} = (\partial C_m / \partial q)_{q=0}. \tag{8}$$

Later, taking into account the more realistic characteristics of the nonsteady flow associated with the aircraft motion, the results received refused both assumptions of Bryan. The new models introduced by Glauert [41] contain additional elements taking into consideration the effect of the past history of the aircraft motion on the current aerodynamic forces and moments [42–44]. The flight dynamic, stability, and control had been applied to Glauert's idea in more general form. The aerodynamic coefficients were defined by the use of c linear air reaction theory outlined by Etkin [41, 45]. In this approach, the coefficients are linearized around the predefined operational points. The interactions between the angle of attack, the control surface deflection, and aerodynamic coefficient, as well as the time lag effect on the aerodynamics, were taken into account. The aerodynamic model was rewritten in form, like the following model of the lift coefficient:

$$\begin{aligned} C_L(t) = \quad & C_{L_0} + C_{L_\alpha}\alpha(t) + C_{L_{\alpha^2}}\alpha^2(t) && + C_{L\dot{\alpha}}\dot{\alpha}(t) && + C_{L_\delta}\delta(t) \\ & \textit{linear part} && + \textit{non} - \textit{linear part} + \textit{time lag} && + \textit{control effect}. \end{aligned} \tag{9}$$

Here $C_{L\dot{\alpha}} = (\partial C_L / \partial \dot{\alpha})_{\dot{\alpha}=\dot{\alpha_0}}$ is the derivative of the lift coefficient, respectively, to the rate of change in angle of attack $\dot{\alpha} = \partial\dot{\alpha}/\partial t$ and it represents the time lag addition determined by using the assumption that it is proportional to $\dot{\alpha}$. The partial derivatives of the aerodynamic models are used as stability derivatives [13–15, 42, 45, 46] and they must be multiplied by changes in variables $\left(\Delta\alpha, \Delta\alpha^2, \ldots\right)$ as deviations from the flight regime (operational point) at which the coefficients are determined. The derivatives should be independent. Principally, quantities $\alpha$ and $\dot{\alpha}$ are not independent. So the models like (9) approximate the aerodynamic coefficient in the form of a mathematically incorrect expansion [11].

## 5. Classic aerodynamic models

The simplified aerodynamic coefficient representations adapted to the real situations and real problems today are the widely and most used aerodynamic models. The different types of simple classic aerodynamic models [1–8, 13–15, 42–46] are shown in **Table 1**.

The usual linearized formulations of the aerodynamic models and nonlinear models described above can only be used for detailed investigations where the aircraft motion is prescribed. This is the mean difficulty with such models.

| Coefficients | Models | Remarks |
|---|---|---|
| $C_L(t)$ | $C_{L_0} + C_{L_\alpha}\alpha(t) + C_{L_{\delta_e}}\delta_e(t)$<br>$C_{L_0} + C_{L_\alpha}\alpha(t) + C_{L_{\alpha^2}}\alpha^2(t) + C_{L_{\delta_e}}\delta_e(t)$<br>$C_{L_0} + C_{L_\alpha}\alpha(t) + C_{L_{\alpha^2}}\alpha^2(t) + C_{L_{\dot\alpha}}\dot\alpha(t) + C_{L_{\delta_e}}\delta_e(t) + C_{L_{\dot\delta_e}}\dot\delta_e(t)$<br>$C_{L_0} + C_{L_\alpha}\alpha(t) + C_{L_{\alpha^2}}\alpha^2(t) + C_{L_{\dot\alpha}}\dot\alpha(t) + C_{L_{\delta_e}}\delta_e(t) + \quad C_{L_{\dot\delta_e}}\dot\delta_e(t)$<br>$+C_{L_{\alpha\delta_e}}\alpha\delta_e(t) + C_{L_{\dot\alpha\delta_e}}\dot\alpha\delta_e(t) + \ldots$ | Simple, linearized model, simple, nonlinearized model (longitudinal motion), model used for nonsteady state aerodynamics, full model |
| $C_D(t)$ | $C_{D_0} + C_{D_V}V(t) + C_{D_q}q(t) + C_{D_\alpha}\alpha(t) + C_{D_{\delta_e}}\delta_e(t)$<br>$C_{D_0} + C_{D_V}V(t) + C_{D_q}q(t) + C_{D_\alpha}\alpha(t) + C_{D_{\alpha^2}}\alpha^2 + C_{D_{\dot\alpha}}\dot\alpha(t)$<br>$+C_{D_{\delta_e}}\delta_e(t) + C_{L_{\dot\delta_e}}\dot\delta_e(t)$<br>$C_{D_0} + C_{D_V}V(t) + C_{D_q}q(t) + C_{D_\alpha}\alpha(t) + C_{D_{\alpha^2}}\alpha^2 + C_{D_{\dot\alpha}}\dot\alpha(t)$<br>$+C_{D_{\delta_e}}\delta_e(t) + C_{L_{\dot\delta_e}}\dot\delta_e(t) + C_{D_{\alpha\delta_e}}\alpha\delta_e(t)$<br>$+C_{D_{\dot\alpha\delta_e}}\dot\alpha\delta_e(t) + C_{D_{\delta_r}}\delta_r(t) + \ldots$<br>$C_{D_0} + C_{D_\alpha}\alpha(t) + C_{D_{\alpha^2}}\alpha^2(t) + C_{D_{\alpha^4}}\alpha^4(t) + C_{D_\beta}\beta(t) + C_{D_q}q(t)$ | Simple, linearized model, simple, nonlinearized model, full model, special model for high angle of attack situations |
| $C_m(t)$ | $C_{m_0} + C_{m_V}V(t) + C_{m_q}q(t) + C_{m_\alpha}\alpha(t) + C_{m_{\delta_e}}\delta_e(t)$<br>$C_{m_0} + C_{D_M}M(t) + C_{D_{M^2}}M^2 + C_{m_q}q(t) + C_{m_{\alpha M}}\alpha M(t) + C_{m_{\alpha^2}}\alpha^2(t)$<br>$+C_{m_{\delta_e}}\delta_e(t) + C_{m_{\varphi_s}}\varphi_s(t) + C_1\frac{\Delta x_{cg}}{C_a} + C_2\frac{\Delta y_{cg}}{C_a}$<br>$C_{m_0} + C_{m_\alpha}\alpha(t) + C_{m_{\alpha^2}}\alpha^2(t) + C_{m_{\alpha^3}}\alpha^3(t) + C_{m_\beta}\beta(t) + C_{m_q}q(t)$<br>$+C_{m_{\delta_e}}\delta_e(t)$<br>$C_{m_0} + C_{m_\alpha}\alpha(t) + C_{m_{\alpha^2}}\alpha^2(t) + C_{m_{\beta^2}}\beta^2(t) + +C_{m_q}q(t) + C_{m_{\delta_e}}\delta_e(t)$<br>$+C_{m_{\alpha\delta_e}}\alpha\delta_e(t)$ | Simple model, model applied to study the required fuel consumption, models for investigation of the nonlinear effects |

Here $\delta_e$ and $\delta_r$ are the deflection angle of the control surface elevator and rudder, $q$ is the dynamic pressure, $\beta$ is the sideslip angle, i.e., angle between the x axes of the body and wind reference systems, and $\Delta x_{cg}$ and $\Delta y_{cg}$ are the coordinates of deviated position of the center of gravity.)
*Remarks.* Often small $c$ is used instead of capital $C$ in aerodynamic coefficients. Sometimes $m_z$ is applied instead of $C_m$.

**Table 1.** Different aerodynamic models and their possible applications.

The full aerodynamic description of the aircraft requires a lot of component models. These models are often defined as semiempirical models, such models are based on theoretical bases, adapted to measured data. **Figure 10a** shows an example for use of such methods developed for aircraft aerodynamic design. The derivative coefficient of the lift generated on the nose part of a fuselage depends on the flight Mach number ($M_\infty$) and ratio of lengths of central and nose parts of the fuselage.

Another example is the calculation of the fuselage friction drag coefficient appearing at zero angle of attack:

$$C_{D_{0,f}} = C_f \eta_t \eta_M \frac{S_{fus_{wet}}}{S_{fus_M}} \tag{10}$$

where $C_f$ is the skin friction drag coefficient thin plate, $\eta_t$ *and* $\eta_M$ are coefficients taking into account the effect from body thickness and flow velocity, $S_{fus_{wet}}$ *and* $S_{fus_M}$ are the fuselage

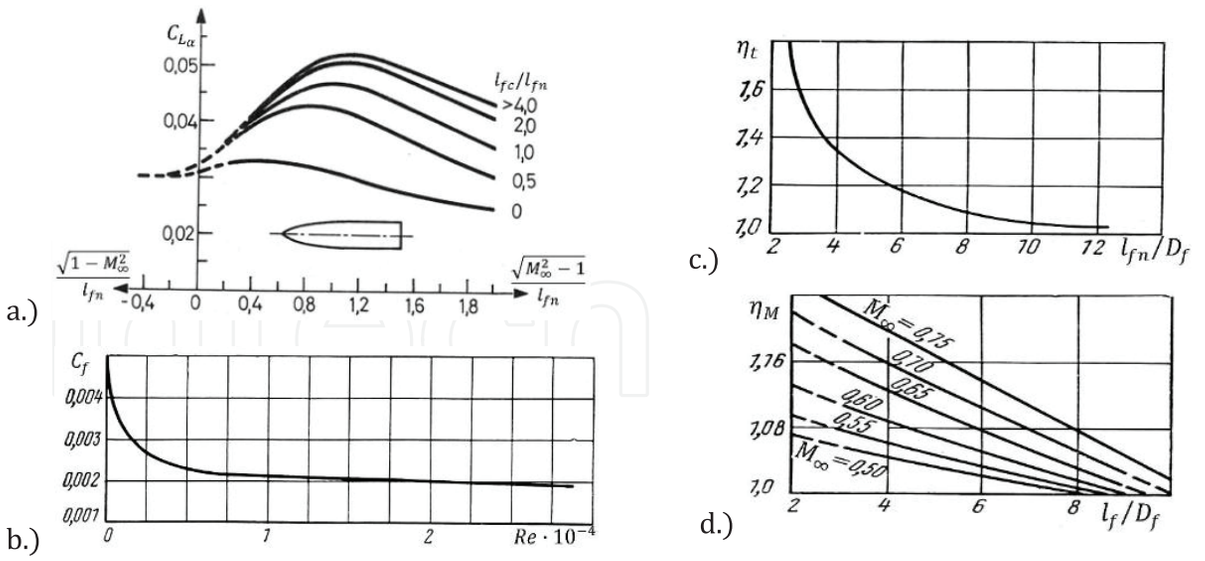


**Figure 10.** Practical figures supporting the estimation and evaluation [5] of the aerodynamic coefficients: (a) lift slop coefficient for estimation of the lift generated on the fuselage nose, (b)–(d) figures defining the estimation of the friction drag generating on the fuselage.

so-called surface wetted area and area of the fuselage mean (maximum) cross-section area, and $D_f$, $l_f$, *and* $l_{fn}$ are the mean diameter, length of fuselage, and length of the nose section of the fuselage (in **Figure 10**). The $C_f$, $\eta_t$, *and* $\eta_M$ coefficients can be estimated from **Figure 10b–d**, while the fuselage wetted area can be calculated with the use of the following formulas:

$$S_{fus_{wet}} = \pi D_f l_f \left(1 - \frac{2D_f}{l_f}\right)^{2/3} \left(1 - \frac{2D_f^2}{l_f^2}\right) \text{if the } {}^{l_f}/_{D_f} \geq 4.5 \text{ or } S_{fus_{wet}} = 2.53 D_f l_f. \tag{11}$$

As it had been outlined already, the first simplified models were adapted to the wide flight dynamics, stability, and control investigations and to the different form of aircraft [13–15, 42–46]. The modern control introduced the state space representation of the linearized system of equations describing the aircraft spatial motion:

$$\dot{\mathbf{x}} = \mathbf{A}\mathbf{x} + \mathbf{B}\mathbf{u} \tag{12}$$

**x** and **u** are the state and control (input) vectors, while **A** and **B** are the state and control matrices. In simplified case, when the aircraft is modeled as rigid body, the state vector contains the components of the linear and rotational (angular) velocities – $\mathbf{x} = [u, v, w, p, q, r]^T$. The control vector is composed of control inputs including the control surfaces' deflection, deflections of other moving elements as flaps, slat, as well as the changes in trust: $\mathbf{u} = \left[\delta_e, \delta_r, \delta_a, \delta_f, \delta_s, \ldots, n_T\right]^T$. Here the control elements are the deflection angle of elevator, rudder, aileron, flaps, slats, and engine revolution speed. Principally, because of the linearization, the state and control vectors contain the changes in velocity components and deflection angles related to the operational (initial) condition. Because of symmetry, the motion equations can be divided into two subsystems: longitudinal and lateral motion. The state vector of the

longitudinal motion model (motion of aircraft in the vertical plane, only) contains the $u$, $w$, $q$ and additionally the pitch (or climb) angle, $\theta$. The **A** and **B** elements are special derivative coefficients.

The aircraft longitudinal motion can be modeled by

$$\begin{aligned} m\frac{du}{dt} &= T\cos(\alpha+\varphi_T) - D - W\sin\theta \\ m\frac{dw}{dt} &= T\sin(\alpha+\varphi_T) + L - W\cos\theta\,. \\ I_y\frac{dq}{dt} &= M \end{aligned} \tag{13}$$

equations that are defined in body system of reference. Here $m$ and $W$ are the aircraft mass and weight, $T$ is the trust and $\varphi_T$ is the engine built angle, angle between the trust direction, $x_b$ is the axis of the body system of reference, and $I_y$ is the inertia moment component. Supposing the $\cos(\alpha+\varphi_T)\approx 1$, $\sin(\alpha+\varphi_T)\approx 0$ and taking into account the $X$, $Z$, and $M$ are the components of the total forces and moment component due to $x$, $z$, and $y$ axes, respectively, Eq. (13) can be rewritten into the space state representation form:

$$\begin{bmatrix} \dot{u} \\ \dot{w} \\ \dot{q} \\ \dot{\theta} \end{bmatrix} = \begin{bmatrix} \frac{X_u}{m} & \frac{X_w}{m} & -g\cos\theta_0 & 0 \\ \frac{Z_u}{m} & \frac{Z_w}{m} & -g\sin\theta_0 & 0 \\ \frac{M_u}{I_y} & \frac{M_w}{I_y} & \frac{M_q}{I_y} & 0 \\ 0 & 0 & 1 & 0 \end{bmatrix} \begin{bmatrix} u \\ w \\ q \\ \theta \end{bmatrix} + \begin{bmatrix} \frac{X_{\delta_e}}{m} & \frac{X_{n_T}}{m} \\ \frac{Z_{\delta_e}}{m} & \frac{Z_{n_T}}{m} \\ \frac{M_{\delta_e}}{I_y} & \frac{M_{n_T}}{I_y} \\ 0 & 0 \end{bmatrix} \begin{bmatrix} \delta_e \\ n_T \end{bmatrix}. \tag{14}$$

Here, the components $X_u$, $X_w$, …, $M_u$, …, $M_q$, are called stability derivatives and $X_{\delta_e}$, …, $M_{n_T}$ are the control derivatives. Of course, the aerodynamic total forces and moments might be estimated by the sum of the derivatives of the force and moment components relevant to the given state and control vector elements.

For instance, $X_u$ should be determined from the first equation of (13):

$$\begin{aligned} m\frac{du}{dt} &= T(V,\Omega,\delta_e,n_T) - C_D\frac{\rho V^2}{2}S - W\sin\theta \\ mX_u &= \frac{\partial T}{\partial u} - \frac{\rho V_0^2}{2}\frac{\partial C_D}{\partial u} - C_D\frac{\rho S}{2}\frac{\partial V^2}{\partial u}, \end{aligned} \tag{15}$$

and in simple case, when $V = u$, the dimension-less derivative equals to:

$$X_u = \frac{T_u}{\frac{\rho V_0 S}{2}} - V_0 C_{D_V} - 2C_D. \tag{16}$$

The drag coefficient, $C_D$, can be represented by the models described earlier.

The static and dynamic stability, flight dynamics (as maneuvers, maneuverability, departure to the critical regimes, and recovery from there) and control design, and control synthesis are required to know the aerodynamic characteristics of the aircraft elements and aircraft devices, too. For instant, the hinge moment coefficient (m) of the control surfaces (elevator, rudder, and ailerons) can be represented by the following simplified models:

$$\begin{aligned} m_e &= m_{e_\alpha}\alpha + m_{e_{\delta_e}}\delta_e + m_{e_{\delta_e T}}\delta_{eT} \\ m_r &= m_{r_\beta}\beta + m_{r_{\delta_r}}\delta_r + m_{r_{\delta_r T}}\delta_{rT} \\ m_a &= m_{a_\alpha}\alpha + m_{a_p}p + m_{a_{\delta_a}}\delta_a + m_{a_{aT}}\delta_{aT} \end{aligned}, \tag{17}$$

where index $T$ depicts the trim tabs and the $p$ is the pitch rate.

Finally, another excellent example demonstrates the interaction between the different theories. As **Figure 8b** shows, the lift coefficient on the delta wing depends on the vortex generated at the leading edge. Polhamus [47] created and explained a special formula for lift coefficient calculation:

$$C_{L_{\Delta w}} = K_p \ sin \ \alpha \ cos^2\alpha + K_V \ cos \ \alpha \ sin^2\alpha \tag{18}$$

Here the first part comes from the small angle of attack potential lifting surface theory. The $K_p$ is the lift curve slop, $sin \ \alpha$ accounts for true boundary condition, and the $cos^2\alpha$ arises from the Kutta-type condition at the leading edge. In second part of the formula (18), the $K_V \ sin^2\alpha$ gives the potential flow leading edge suction, i.e., vortex normal force, and the $cos \ \alpha$ defines its component in the lift direction.

The classic models are well applied in identifying them from flight data and developing the flight simulation methods, too [29, 48].

## 6. Developed aerodynamic models

The classic aerodynamic models cannot be applied to accurate description of the aircraft motion at high angle of attack, aircraft maneuvers, dynamic, oscillation motion or aerodynamic characteristics in flutter, etc. Tobak [49] introduced a model structure. He made a special assumption: the changes in aerodynamic coefficients are linear functions of changes in variables that are independent of the past history of these variables, namely on all values that these variables have taken over the course of the motion prior to time $\tau$. For example, the change in pitching moment can be defined by following functions:

$$\Delta C_m = \frac{\Delta C_m(t-\tau)}{\Delta\delta}\Delta\delta + \frac{\Delta C_m(t-\tau)}{\Delta(ql/V)}\Delta(ql/V) \tag{19}$$

Here $\delta$ is the motion of aircraft along the $z$ axis in body axis system ($\delta = z$), $q$ is the angular velocity around the $y$ axis, and the derivatives depend on elapsed time $t$ -$\tau$ rather than on $t$ and $\tau$.

The derivatives in Eq. (19) come from solution of linear equation of gas dynamics. However, the linearity assumption does not rest on the assertion that change in pitching moment, ($\Delta C_m$),

is linear dependent on changes in variables, $\Delta\delta(=\Delta\delta_e)$ and $\Delta(ql/V)$. So, these two increments must not be linear additives in Eq. (19).

Principally, the aerodynamic pitching moment coefficient response to variations $\delta$ and $q$. These variations can be broken into a large number of small step changes (**Figure 11**). No matter how large the values of $\delta$ and $q$ at the beginning of steps, the derivatives depend on the $t$ -$\tau$, only. The limits of these functions

$$\lim_{\Delta\delta\to 0}\frac{\Delta C_m(t-\tau)}{\Delta\delta}=C_{m_\delta}(t-\tau),\qquad \lim_{\Delta(ql/V)\to 0}\frac{\Delta C_m(t-\tau)}{\Delta(ql/V)}=C_{m_q}(t-\tau) \tag{20}$$

are called as the linear indicial pitching moment responses per unit step changes in $\delta$ and $ql/V$, respectively [11, 49].

Using this indicial function concept to calculate the aerodynamic coefficients, Tobak [11, 49] replaced Bryan's function with a linear functional in the form of the linear superposition integral like:

$$C_m(t)=C_m(0)+\int_0^t C_{m_\delta}(t-\tau)\frac{d}{d\tau}\delta(t)\mathrm{d}\tau+\frac{1}{V}\int_0^t C_{m_q}(t-\tau)\frac{d}{d\tau}q(t)\mathrm{d}\tau. \tag{21}$$

In reality, the functions of aerodynamic coefficient and derivatives depend on all the past values of the motion variables. In accordance to Volterra's description, the aerodynamic coefficient as function can be given in the form of a functional:

$$C_m(t)=\mathrm{G}[\delta(\xi),q(\xi)] \tag{22}$$

Generally, the whole time/past history of motion variables is unknown. Therefore, the functional (22) can be replaced by a functional describing the dependence on the past in the form of analytical functions in the neighborhood of $\xi=\tau$ reconstructed from the Taylor series expansions of the coefficients about $\xi=\tau$. This obtains for example:

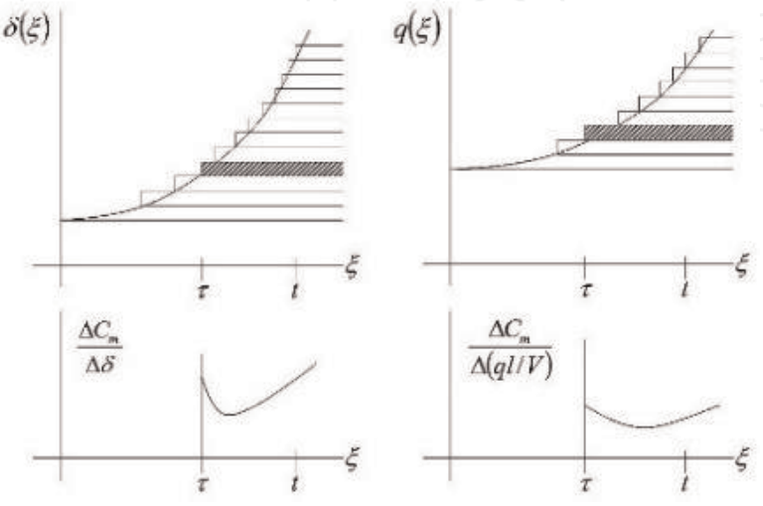


**Figure 11.** Simulation of incremental responses.

$$C_{m_\delta}[\delta(\xi), q(\xi); t, \tau] = C_{m_\delta}\left(t, \tau; \delta(\tau), \dot{\delta}(\tau), \ldots, q(\tau), \dot{q}(\tau), \ldots\right). \tag{23}$$

Hence, at most, only the first few coefficients of expansions of $\delta(\xi)$ and $q(\xi)$ need be retained to characterize correctly the most recent past [49], which is all the indicial response remembers. Using the two coefficients of $\delta(\xi)$, for example, implies matching the true past history of $\delta$ in magnitude and slope at the origin of the step, thereby approximating $\delta(\xi)$ by a linear function of time

$$\delta(\xi) \approx \delta(\tau) - \dot{\delta}(\tau)(\tau - \xi). \tag{24}$$

With application of this approach. Eq. (21) can be rewritten into the following form:

$$\begin{aligned} C_m(t) = C_m(0) &+ \int_0^t C_{m_\delta}\left(t, \tau; \delta(\tau), \dot{\delta}(\tau), q(\tau), \dot{q}(\tau)\right) \frac{d}{d\tau}\delta(t)\mathrm{d}\tau \\ &+ \frac{1}{V}\int_0^t C_{m_q}\left(t, \tau; \delta(\tau), \dot{\delta}(\tau), q(\tau), \dot{q}(\tau)\right) \frac{d}{d\tau}q(t)\mathrm{d}\tau \end{aligned} \tag{25}$$

This method of model definition is more attractive then (21) and gives the possibility of taking into account the considerable nonlinearities, time lag, and hysteresis, too. All the developed models follow from this model formation. For example, in case of slowly varying motion, Eq. (25) may be formalized in a more general form,

$$C_m(t) = C_m(0) + \int_0^t C_{m_\delta}(t - \tau; \delta(\tau), q(\tau)) \frac{d}{d\tau}\delta(t)\mathrm{d}\tau + \frac{1}{V}\int_0^t C_{m_q}(t - \tau; \delta(\tau), q(\tau)) \frac{d}{d\tau}q(t)\mathrm{d}\tau \tag{26}$$

still capable of embracing a fairly broad range of nonlinear problems of aerodynamics.

The use of indicial aerodynamic functions is a rather complex task even for 2D [50].

The next step in developing the aerodynamic models was made by Goman and his colleague [51, 52]. They had formulated the aerodynamic coefficient models in the form of a state space representation:

$$C_a = C_a(\boldsymbol{\xi}(t)\boldsymbol{\eta}(t)), \tag{27}$$

where

$$\dot{\boldsymbol{\eta}}(t) = \mathbf{g}\left(\boldsymbol{\eta}(\boldsymbol{t})\boldsymbol{\xi}(\boldsymbol{t})\dot{\boldsymbol{\xi}}(\boldsymbol{t})\right) \tag{28}$$

and

$$\boldsymbol{\xi}(t) = \left[\boldsymbol{x}(t)^T \boldsymbol{u}(t)^T\right]^T. \tag{29}$$

Here $\boldsymbol{\eta}$ is an internal additional state vector and $\mathbf{x}$ and $\mathbf{u}$ are the state and control vectors from the aircraft motion models (see Eq. (12)). For instance, Ref. [51] described the aircraft longitudinal dynamics by introducing the internal state variable representing the vortex burst point location along the chord of a triangular wing.

## 7. Advanced aerodynamic models

The collection of large databases of practical wind tunnel and flight test measurements and wide use of rapidly developing methods of computational fluid dynamics and a series of new methods have developed for modeling the aerodynamic coefficients. Three different approaches can be applied: (i) approximation and interpolation, (ii) analytical models and special models, and (iii) models developed using soft computing models.

The polynomial, and trigonometric interpolation, spline or regression models can be used for determining the aerodynamic coefficients or aerodynamic forces directly. For example, reference [53] uses the Lagrange interpolation to determine the lift and drag coefficient when studying the takeoff taxiing. The piecewise cubic Hermite interpolating polynomial and Spline are applied [54] to calculating the derivative of the pressure distribution on airfoil for determining the laminar-to-turbulent transition. The transition is identified as the location of maximum curvature in the pressure distribution. The Chebyshev polynomials and their orthogonality properties were applied [55] for approximation of unsteady generalized aerodynamic forces from the frequency domain into the Laplace domain, acting on a Fly-By-Wire aircraft. The results were compared with Padé method and validated on the aircraft test model.

The oscillation in changes of the aerodynamic forces and their coefficients contributes to the most interesting areas of developing the aerodynamic coefficient models. This area has two major parts: (i) oscillation of the aircraft elements, like flutter, and (ii) oscillation flight of aircraft. The first and today valued as fundamental studies were published in 1920s and 1930s. Wagner [56] dealt with unsteady lift on airfoil due to abrupt changes in angle of attack and he calculated the circulation around the airfoil in response to a step in angle of attack. Theodorsen [57] extending the Wagner concept developed a model for quasi-steady thin airfoil theory including added-mass forces and the effect of wake vorticity.

$$C_L = \pi\left[\ddot{h} + \dot{\alpha} - a\ddot{\alpha}\right] + 2\pi\left[\alpha + h + \alpha\left(\frac{1}{2} - \alpha\right)\right]C(k) \tag{30}$$

Here the added-mass force taken into account by the first addend, while the second one defines the quasi-steady lift from thin airfoil theory by a transfer function C(k) as lift attenuation by the wake vorticity. The $h$ is the vertical position of airfoil, $a$ is the pitch axis with respect to 1/2 chord, and the Theodorsen's transfer function C(k) is expressed in terms of Hankel functions:

$$C_L(k) = \frac{H_1^{(2)}(k)}{H_1^{(2)}(k) + iH_0^{(2)}(k)}, \tag{31}$$

where $H_n^{(2)}(k) = J_n - Y_n, \quad n = 0, 1$ are Bessel function, and $k = \omega c/2V_\infty$, where ω is the motion frequency, c is the airfoil chord, and $V_\infty$ is the free stream velocity. This approach is well applicable nowadays, too (see [58, 59]).

In 1980s and 1990s during the development of the supermanoeuvrable and thrust vectored aircraft, the hysteresis in aerodynamic coefficient was intensively studied. These aircrafts fly at critical regimes, near or at the border of the flight envelopes. Thrust vectored aircraft uses the controlled poststall flights.

The hysteresis effects in aerodynamic coefficients can appear in different forms depending on the oscillation frequency [60–63]. **Figure 12** shows typical hysteresis caused by stall in normal force coefficient at the high angle of attack flight [64] and in steady-state pitching moment response [65].

The considerable nonlinearities in the aerodynamic coefficients that generate the hysteresis in aerodynamic characteristics near the critical angle of attack in stall and poststall domain, of course, are well investigated by practical methods in wind tunnels [66–69].

The formation of flow separation at the critical angle of attack is a quite complete process [70], and the hysteresis [64] shown in **Figure 12a** fundamentally depends on the frequency of changes in the angle of attack. Therefore, the approximation of these characteristics is a difficult task. The models described earlier cannot ensure the required accuracy in the full region of parameter variations. The aerodynamic models used in the early works were based on fitting polynomials [71] or cubic [72, 73] or bi-cubic [74, 75] splines as interpolation schemes for measured data given in the form of table. In some cases [76], the methods that worked out for bifurcation analysis did not require further smoothing and the linear interpolation had been applied.

In many cases, the aerodynamic coefficients are given in table form [68, 69] or directly estimated from the flight tests [29, 77]. Data can be obtained by special analytical models [78]:

$$C_F = b_0 + \sum_{i=1}^{n} b_i arctan((\alpha - c_i)d_i), \tag{32}$$

where $b_0$, $b_i$, $c_i$ are the constants.

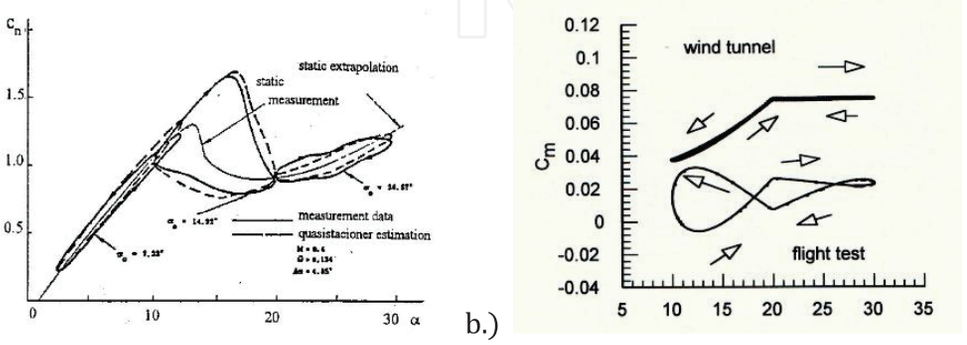


**Figure 12.** Typical hysteresis in aerodynamic coefficients. (a) At high angle of attack [64], (b) moment coefficient estimated from the wind tunnel and flight test of F-16XL-1 [65] (at reduced frequency $k$ = 0.054).

http://dx.doi.org/10.5772/intechopen.71419

This model was developed especially for the approximation [78] of experimental data received from wind tunnel investigations [68, 69]. The aerodynamic models obtained in form (32) can be used in full AoA region from −10 to 90°. Analytical models of type (32) have a great advantage; namely, there is no $\alpha$ value, where the derivative of this function does not exist.

**Figure 13** shows some examples of developed analytical models defined for different speeds and elevator deflections with linear approximation between them. One example of these NASA-backed representation of the actual derivative involves four to eight arcus tangent functions:

$$C_{m\dot{\alpha}} = -\frac{0.02}{\pi} arctg\left(-5\pi\frac{\alpha-1}{18}\right) + 0.5\, arctg(5(\alpha-6)) - 0.8 arctg\left(\frac{\alpha-18}{2}\right) + 0.9 arctg\left(\frac{\alpha-45}{2}\right) - 0.9 \tag{33}$$

Since 1990s, by developing numerical aerodynamics, and applying the methods of soft computing, new types of aerodynamic coefficient representations have been developed. It seems the most applied method is based on using the neural network [79, 80]. The other papers predicted the aerodynamic coefficient of transport aircraft with the use of artificial neural networks [81], simulated the dynamic effects of canard aircraft aerodynamics [82], used genetic algorithm optimized neural networks for predicting the practical measurements [83], determined the global aerodynamic modeling with multivariable spline [84], and applied the fuzzy logic modeling to the aircraft model identification [85] and nonlinear unsteady aerodynamics [86]. Principally all the numerical methods might be applied. For instance, the aircraft stability and control can be modeled with the use of wavelet transforms [87] or even the computed stability derivatives can be applied directly in aerodynamic shape optimization [88]. Nowadays, the computer capacity and sizes allow to use the real-time on-board identification of the nonlinear aerodynamic models [89].

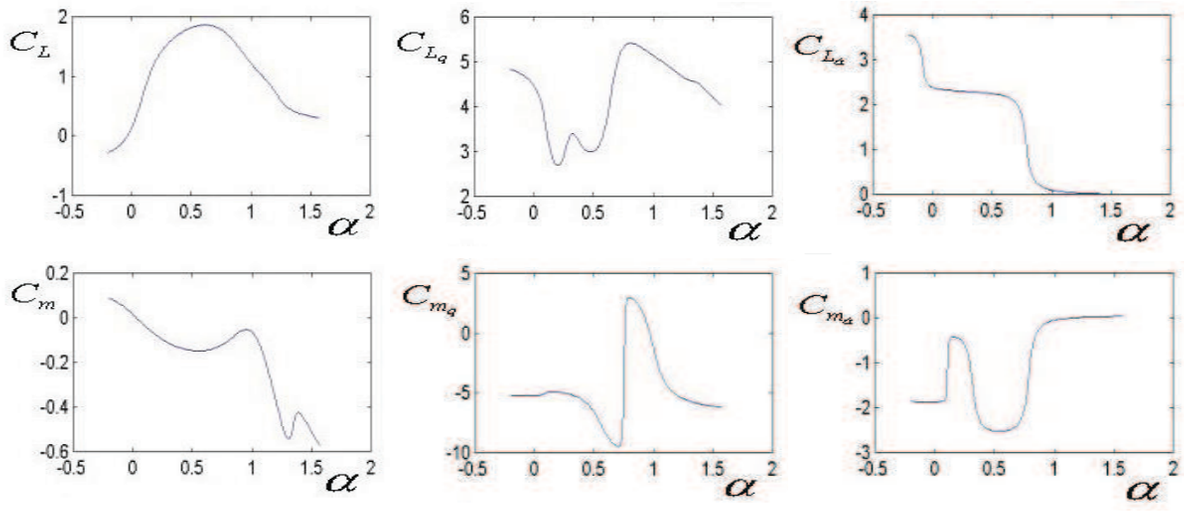


**Figure 13.** Several analytical models (lift and pitching moment coefficients and their derivatives, respectively, to pitch rate and rate of angle of attack) defined by [78].

Two specific aspects must be underlined: (i) the computational fluid dynamics may easily determine the aerodynamic coefficients by integration of the calculated surface pressure distribution and (ii) all the aerodynamic coefficient models described earlier can be applied, while better using the models as simple as possible depending on the goal and object of their application.

## 8. Applicability of the aerodynamic coefficient models

**Table 1** has given already some advises for possible application of the different models of the aerodynamic coefficients. The developed and advanced models open new fields of application including the investigation of the fully nonlinear situations including the aircraft chaotic motions and provide more accurate derivatives for maintaining stability and control.

The model application is based on the known technology identification, evaluation, and selection methodology [90, 91]. This methodology can be adapted to the aerodynamic coefficient model selection by using the following major steps:

**1.** Definition of the object, objectives, and goals

Define the object as thrust vectored aircraft, wing flutter, and objectives like managing the thrust vectored aircraft poststall motion, or reducing the amplitudes of the wing oscillation motion. Derive the goals from the objectives as investigation, design the new system, and control or manage with the object, etc.

**2.** Identification of the applicable models

Derive the preliminary specification of the required models for the definition of the object, objectives, and goals. Namely, the models might be local (used locally to a part of the aircraft or to well-defined motion regime, like cruise flight, only) or global (applying to the whole aircraft, or to the large part of flight envelope). Estimate which nonlinearities, delay, and hysteresis in aerodynamic coefficient may appear that should be taken into account.

Identify the possible models from literature review, preliminary investigations, brainstorming, etc.

**3.** Evaluation of the identified models

Study the identified models: especially evaluate how they can be integrated into the existing or planned systems (compatibility), how their changes or modification may improve their applicability for supporting the objectives (apply the morphological matrix), how their deployments have impact on the applying systems (impact matrix—effect on the solutions like using the different control philosophy and control technique), how effective, safe, sustainable, etc. is their application, and how they might have influence on their selection (decision matrix).

The evaluation must be dealt with development of the final systems, including the production, supply chain, market introduction, etc.

The candidate models might be tested in simulation, or even in laboratory or flight tests. The tests must cover the full range of possible flight regimes and situations, and the result must be evaluated against the predefined indicators. The sensitivity analysis may detect the most important parts or elements of the models.

4. Selection of the best models for the aerodynamic coefficients required for reaching the predefined objectives

   The selected models must be as simple as possible, while their application is (life cycle) cost-effective and they must support the objectives.

5. Development of the systems applying the selected aerodynamic coefficient models

   The system developments include the hardware and software developments and a study of the total impact (effect on the life cycle cost, safety, security, and environment as chemical emissions and noise) and verification and validation of the created systems.

6. Final decision and deployment

   Depending on the previous points, the identification, evaluation, and selection process might be finished or started from the beginning. Of course, with the changes in aircraft structures, new ways of operation, application of the new solutions, and new emerging technologies, the aerodynamic coefficient models always must be refined or even the identification, evaluation, and selection process must be repeated again and again followed by improving or developing new solutions and systems improving the aircraft aerodynamic shape, aerodynamic characteristics, performance, stability, disturbed motion, and controllability.

**Table 2** gives some advises on how to use the different models of the aerodynamic coefficients.

| Models | Typical examples | Applicability |
|---|---|---|
| Simple | $C_L = C_{L_0} + C_{L_\alpha}\alpha(t) + C_{L_{\delta_e}}\delta_e(t) C_D = C_{D_0} + C_{D_\alpha}\alpha(t) + C_{D_{\alpha^2}}\alpha^2$ | Local models for simplified cases like drag-required thrust-fuel consumption for cruise flight, studying the linearized static motion static stability |
| Classic | $C_L = C_{L_0} + C_{L_\alpha}\alpha(t) + C_{L_{\alpha^2}}\alpha^2(t) + C_{L\dot{\alpha}}\dot{\alpha}(t) + C_{L_{\delta_e}}\delta_e(t) + C_{L_{\dot{\delta}_e}}\dot{\delta}_e(t)$ | Static, queasy static models for full range of flight envelope including the high angle of attack flights, linearized motion equations, semiempirical models defining the stability and control derivatives, basic unsteady models |
| Advanced | $C_m(t) = C_m(0) + \int_0^t C_{m_\delta}(t-\tau)\frac{\mathrm{d}}{\mathrm{d}\tau}\delta(t)\mathrm{d}\tau + \frac{1}{V}\int_0^t C_{m_q}(t-\tau)\frac{\mathrm{d}}{\mathrm{d}\tau}q(t)\mathrm{d}\tau$ | Models for dynamic motion, analysis of the critical flights, study and control of dynamic effects including delays, hysteresis in models, etc., developing the global models, critical flights |
| Developed | $C_F = b_0 + \sum_{i=1}^{n} b_i \arctan((\alpha - c_i)d_i),$ | Models for all specific flight situation, and regimes by approximation of the available wind tunnel and/or flight tests measured data, developing models by use of soft computing based on classic or developed models |

**Table 2.** Some recommendations on the usage of the aerodynamic coefficient models.

## 9. Example of use of an advanced aerodynamic coefficient model

The Department of Aeronautics, Naval architecture and Railway Vehicles at the Budapest University of Technology and Economics (operating two flight simulators, one air traffic management laboratory with several working environment for ATCOs, small gas turbines, water channel, etc.) is active in computational fluid dynamics [92, 93], vehicle design [24, 25, 94], vehicle motion simulation [95, 96], developing original and radically new technologies [97–99], and has worked on investigation of the thrust vectored aircraft motion at high angle of attack in poststall domain [100, 101], approximation of the motion after stall [102], and unconventional and critical flights [103, 104]. One of the excellent applications of the analytical models of the aerodynamic coefficients is their using in bifurcation analysis of the poststall motion of thrust vectored aircraft.

Only the longitudinal motion was investigated. The applied system of equations defined by the use of body axis was reduced to four dimensions given in the following form [101]:

$$\begin{aligned} \dot{u} &= -qw + \frac{X}{M} - gsin\theta + \frac{T_x}{M} \\ \dot{w} &= -qu + \frac{Z}{M} - gcos\theta + \frac{T_z}{M} \\ \dot{q} &= \frac{C_m \overline{q} S c_A + X l_z + Z l_x - T_x L_{xe}}{I_y} \\ \dot{\theta} &= q \end{aligned} \tag{34}$$

where $X = \overline{q}S(C_L sin\alpha - C_D cos\alpha)$, $Z = \overline{q}S(C_L cos\alpha + C_D sin\alpha)$, $C_L = C_{L_0} + \frac{c_A}{2V}\left(C_{L\dot{\alpha}}\dot{\alpha} + C_{L_q}q\right)$, $C_D = C_{D_0} + \frac{c_A}{2V}\left(C_{D\dot{\alpha}}\dot{\alpha} + C_{D_q}q\right)$, $C_m = C_{m_0} + \frac{c_A}{2V}\left(C_{m\dot{\alpha}}\dot{\alpha} + C_{m_q}q\right)$, $T_x = Tcos\delta_{vp}$, $T_x = Tsin\delta_{vp}$. Here X and Z are the force components to x and z axis, M is the pitching moment, $\overline{q}$ are $q$ are the dynamic pressure and pitch rate, respectively, and $T$, $T_x$, and $T_z$ are the thrust and its components.

Different types of simple and classic aerodynamic coefficient models were applied that could not result in stable and acceptable solutions. Therefore, the described system of equations and analytical models of aerodynamic coefficients were filled up by data of F/A-18 aircraft [68, 69, 78]. These models defined the hysteresis effects, as well, and they may be used in full region of the possible changes in angle of attack (see **Figure 13**).

The system of equation was solved by different numerical methods (Runge-Kutta and Adams-Moulton) with different step size. Software MATHLAB and ACSL were used in the simulations. The results received were stable and the same at time steps $10^{-2}$ and $10^{-6}$ s.

**Figure 14** shows the equilibrium surface obtained in the thrust-thrust deflection parameter space (left side) and the bifurcation curves (right side) for flight regime $V$ = 0.3 M and $H$ = 15,000 ft. ($T$ = 22.7 kN, $\delta_{vp} = 0°$).

As it can be seen, the poststall domain of the thrust vectored aircraft motion can be divided into six different subspaces. The subspaces are divided by bifurcations. There were found two

http://dx.doi.org/10.5772/intechopen.71419

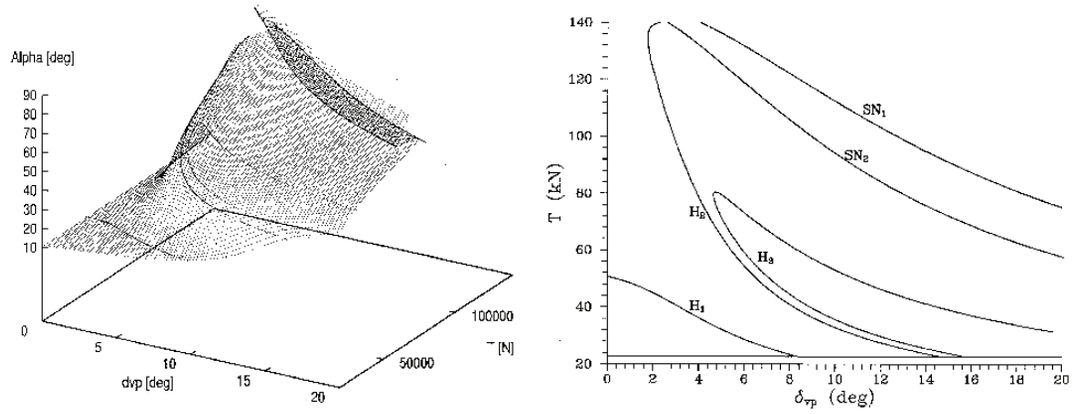


**Figure 14.** Equilibrium surface on the thrust-thrust deflection parameter space (left side) and the bifurcation curves (right side).

different types of bifurcation, e.g., Hopf (H) and saddle-nodes (SN) bifurcations. The first region at the small thrust and small angle of thrust-deflection is characterized the phugoid motion of aircraft before the stall. Oscillation of speed is greater than changes in angle of attack. The fighter slowly returns to the stable position.

As chosen by increasing the thrust and thrust-deflection, the system reads the first Hopf bifurcation ($H_1$) (a small amplitude limit cycle appears at the bifurcation point). Further by increasing thrust and thrust deflection, there is no stable state of the aircraft. Over this second region, changes in the thrust and thrust deflection cause lack of stability before and poststall oscillation of the aircraft. This oscillation tends to the limit cycle and the angle of attack can reach the 90°.

By another Hopf-bifurcation, the system gains back its stability in the poststall regimes. This is the narrow streak area inside the second zone. At high thrust and thrust-deflection, the saddle-node bifurcation (SN) emerges creating jump phenomena. The motion of aircraft in zone appearing after first saddle-node bifurcation curve is an oscillation motion in the poststall domain.

Finally, in the last zone at very high thrust and thrust-deflection, an overpulling appears, when the angle of attack reaches over 90° during the first period of motion after changes in the thrust or thrust deflection.

The bifurcations were followed by continuation method. The input was generated in the thrust deflection (not in the thrust), as it would have been usual nonlinear approach. Components $T_x$, $T_z$ were computed by the following formulas:

$$T_x = T\cos\left(\delta_{vp} + \varepsilon\cos\omega t\right), \qquad T_z = T\sin\left(\delta_{vp} + \varepsilon\cos\omega t\right). \tag{35}$$

In some cases, several interesting changes were found in angle of attack response on oscillation in thrust deflection (**Figure 15**). Little bit nicer representation of this chaotic changes in angle of attack is given in **Figure 16**. This is a 3D phase plot by redrawing of simulation results shown in **Figure 15**. Such phase plot represents the chaos in system output received as results of periodic excitations and it is called as chaotic attractors.

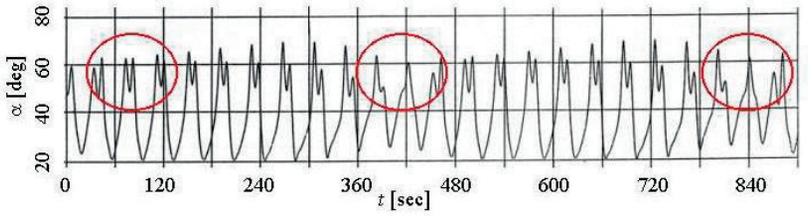


**Figure 15.** Angle of attack response initiated by thrust oscillation with amplitude 2° and frequency 0.33 rad/s applied to initial condition of equilibrium at $T = 35$ kN and $\delta_{vp}=10^0$.

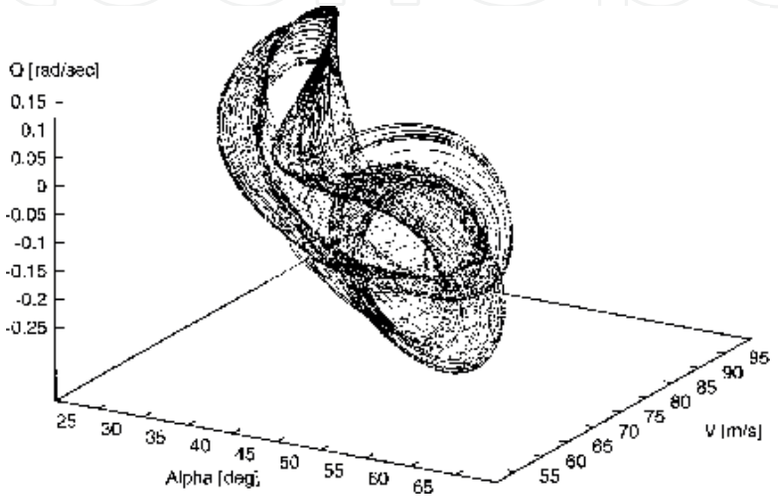


**Figure 16.** 3D phase plot of chaotic attractor is described by simulation results given in **Figure 15**.

A small change in system parameters or in excitations can cause a relatively big change in system output (**Figure 17**). For example, reduction of excitation frequency from 0.33 to 0.32 rad/s involved reduction of chaotic behavior in response and resulted in periodic orbits (see **Figure 17**). In some cases, the periodic orbits are reduced to one (it may be strange) limit cycle. The other figure shows that around 0.9 rad/s another type of noninear phenomenon appears, which is called period doubling bifurcation. At this point, the time period becomes twice as long (no sudden catastrophic change). Decreasing the frequency, a cascade of period doubling bifurcation happens leading to chaos around 0.65 rad/s. **Figure 17** demonstrates several chaotic regions can appear (see chaotic window at the $\omega = 0.35$ rad/s in **Figure 17**).

Further investigation of the aerodynamic coefficient models had been studied by use of sensitivity analysis and changes in structure of the models. The sensitivity analysis had shown that the changes in aerodynamic derivatives for 5 or 1% did not result in considerable changes in response on the applied oscillated thrust deflection.

Using the same mathematical model, initial condition, and excitation (at $T = 35$ kN, $\delta_{vp} = 10$ deg., $\Delta\delta_{vp} = 2$ d° and $\omega = 0.33$ rad/s), the simulations were realized with the use of different aerodynamic coefficient models, in which different parts, or derivatives, were omitted. The results show that elements cause the changes in angle of attack responses (**Table 3**).

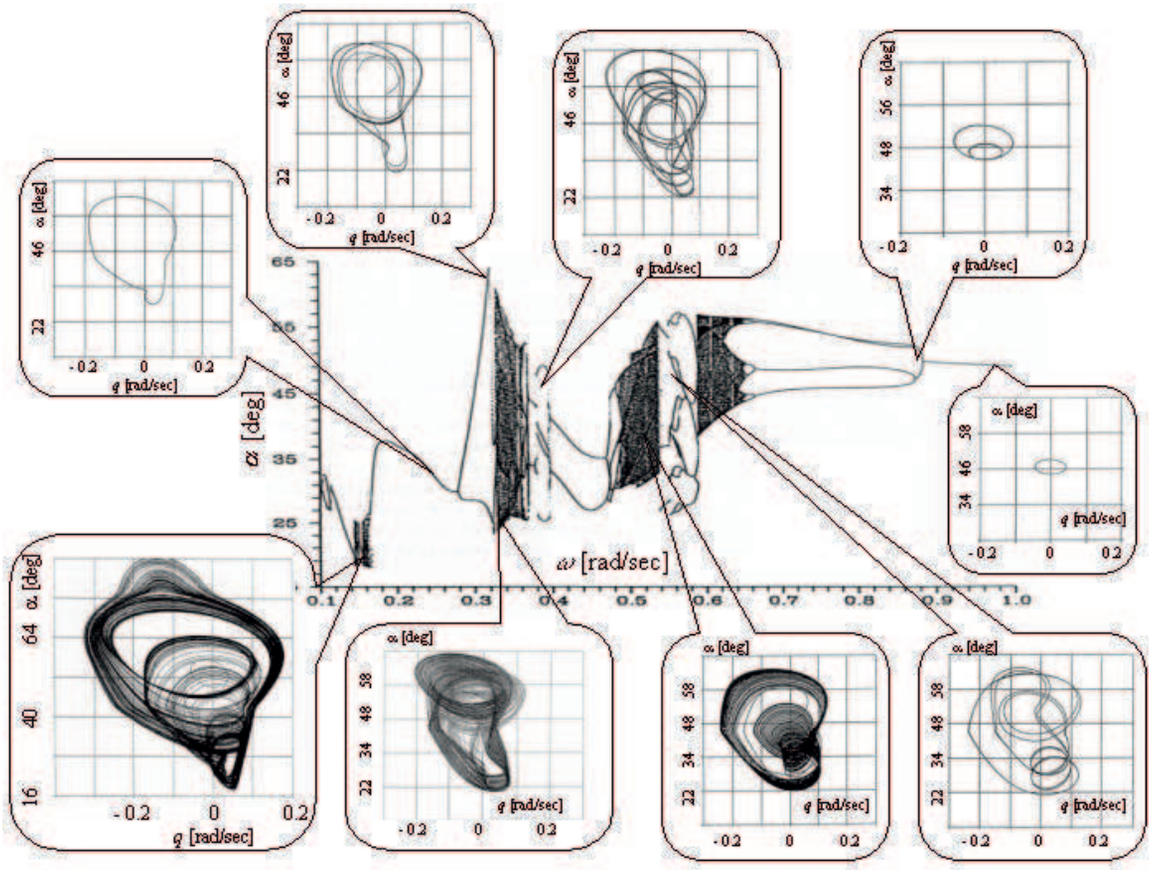


**Figure 17.** Stroboscopic map and different phase plots demonstrate the results of simulation thrust oscillation with amplitude 2° with varied frequency applied to initial condition of equilibrium at $T = 35$ kN and $\delta_{vp}=10^0$.

| $C_{M_q}$ | $C_{M\dot{\alpha}}$ | $C_{L_q}$ | $C_{L\dot{\alpha}}$ | **Remark** | $C_{M_q}$ | $C_{M\dot{\alpha}}$ | $C_{L_q}$ | $C_{L\dot{\alpha}}$ | **Remark** |
|---|---|---|---|---|---|---|---|---|---|
| + | + | + | + | Chaos | — | + | + | + | Limit cycle |
| + | + | + | — | Chaos | — | + | + | — | Limit cycle |
| + | + | — | + | Chaos | — | + | — | + | Limit cycle |
| + | + | — | — | Chaos | — | + | — | — | Limit cycle |
| + | — | + | + | Transient chaos | — | — | + | + | Limit cycle |
| + | — | + | — | Transient chaos | — | — | + | — | Limit cycle |
| + | — | — | + | Transient chaos | — | — | — | + | Limit cycle |
| + | — | — | — | Transient chaos | — | — | — | — | Limit cycle |

**Table 3.** Influence of aerodynamic model structure on the aircraft poststall motion initiated by cosine excitation in thrust deflection angle (sign shows the omitted elements).

## 10. Conclusions

Aerodynamics deals with interaction of air and bodies moving in it. The major task of aerodynamics is to define and describe the aerodynamic forces and moments generated on the bodies.

Because of the very complex ways of causing the aerodynamic forces and moments, the nondimensional aerodynamic force and moment coefficient and series of their models had been developed for the last hundred years. This short chapter tries to show the different aspects having influences on "burning" the aerodynamic forces and moments and their contributing elements.

The aerodynamic coefficient models can be classified as simple, classic, developed, and advanced models. The models use the partial derivative coefficients, indicial step responses, analytical models, interpolation and approximation of the available wind tunnel, flight test, or numerical simulation data, and models are generated by utilization of the soft computing methods.

There is no unique and well-applicable method to selecting the required and best coefficient models. Always the object- and goal-oriented models must be selected. The identification, evaluation, and selection process may use the general methodology: (i) definition of the object, objectives, and goals, (ii) identification of the applicable models, (iii) evaluation of the identified models, (iv) selection of the best models, (v) development of the systems applying the selected aerodynamic coefficient models (including the verification and validation, too), and (vi) final decision.

There are some recommendations supporting the selection of the aerodynamic coefficient models and an example demonstrates using a special model to complex motion of thrust vectored aircraft in poststall domain.

## Author details

Jozsef Rohacs

Address all correspondence to: jrohacs@rea-tech.eu

Budapest University of Technology and Economics, Budapest, Hungary

## References

[1] Anderson DJ Jr. Fundamentals of Aerodynamics. St. Louise, New York: McGraw-Hill Inc.; 1991. 792 pp

[2] Houghton EL, Carpenter PW. Aerodynamics for Engineering Students. Oxford, Amsterdam: Butterworth Heinemann; 2003. 614 pp

[3] Schlichting H, Truckenbrodt E. Aerodynamic des Flugzeugs. 3rd ed. Berlin, Heidelberg, New York: Springer-Verlag; 2001. Teil 1 480 pp, Teil 2 515 pp

[4] Krasnov NF. Aerodinamika (in Russian). 2nd ed. Moscow: Vysshaya Skola; 1976. T1 383 pp, T2 468 pp

[5] Mhitaryan AM. Aeriodinamika (in Russian). Masinostroyeniye: Moscow; 1976. 446 pp

[6] McCormick BW. Aerodynamics, Aeronautics and Flight Mechanics. 2nd ed. New York: John Wiley and Sons., Inc.; 1995. 652 pp

[7] Rohacs J, Gausz ZS, Gausz T. Aerodinamika (in Hungarian). Typotex: Budapest; 2012. 220 pp

[8] McLean D. Understanding Aerodynamics: Arguing from the Real Physics. West Sussex, England: John Wiley and Sons, Inc.; 2013, 550 pp

[9] Rohács J, Gránásy P. Effects of non-linearities in aerodynamic coefficient on aircraft longitudinal motion. In: Sivasundaram S, editor. Non-Linear Problems in Aviation and Aerospace. New York: Gordon and Breach; 2000, pp. 281-296

[10] Rohács J. Bifurcation analysis of aircraft poststall motion. In: Proceedings of the 7th Mini Conference on Vehicle System Dynamics, Identification and Anomalies; Budapest, 2000; Department of Railway Vehicles, BUTE, Budapest. 2001. pp. 53–76

[11] Tobak M, Schiff LB. Aerodynamic Mathematical Modelling—Basic Concepts, Dynamic Stability Parameters. AGARD-LS-114. 1981. pp. 1.1–1.31

[12] Bisplinghoff RL, Ashley H, Halfman RL. Aeroelasticity. Cambridge, MA: Addison-Wesley Publishing Company, Inc.; 1955. 860 pp

[13] Etkin B, Reid LD. Dynamics of Flight, Stability and Control. 3rd ed. New York: John Wiley and Sons, Inc; 1996, 383 pp

[14] Cook MV. Flight Dynamics Principles. London: Arnold; 1997, 352 pp

[15] Stengel R. Flight Dynamics. Princeton University Press; 2004

[16] Szabo J, editor. Aviation lexicon (in Hungarian: Repülési lexikon). Budapest: Akademiai Kiadó; 1991. T.1 and T.2, 623 + 603 pp

[17] Van Dyke M. An Album of Fluid Motion. Stanford: The Parabolic Press; 1982. 174 pp

[18] Prandtl L. Über Flüssigkeitsbewegung bei sehr kleiner Reibung. In: Krazer A, editor. "Verhandlungen des Dritten Internationlen Mathematiker-Kongresses in Heidelberg; August 8–11, 1904; Leipzig: Druck und Verlag von B. G. Teubner; 1905. pp. 484-491

[19] Karman T. Über laminare und turbulente Reibung. ZAMM Zeitschrift für Angewandte Mathematik und Mechanik. 1921;**1**(4):232-252

[20] Schlichting H. Grenzschicht-Theorie. Kalsruhe: Verlag G. Braun; 1965. 736 pp. (Boundary Layer Theory, 7th ed. New York: McGraw-Hill Book Company, Inc.; 1979. 817 pp. [in English])

[21] Versteeg HK, Malalasekera, W. An Introduction to Computational Fluid Dynamics, The Finite Volume Method. 2nd ed. Harlow, London: Pearson, Prentice Hall; 2007. p. 517

[22] Cummings RM, Mason WH, Morton SA, McDaniel DR. Applied Computational Aerodynamics, A Modern Engineering Approach. Cambridge University Press; 2015. 849 p

[23] Charlott JJ, Hafez MM. Aerodynamics: And Related Numerical Methods. Dordrecht, Heidelberg: Springer; 2015. 620 pp

[24] Rohacs J, Voloscsuk A, Gecse T, Ovari Gy. Innovation process management for reducing the time to market. Aerospace—The Global Industry; November 2–4, 2010; Exhibition Centre Frankfurt, Main Germany, Conference Proceedings; AIRTECH GmbH and Co. KG. 2010. p. 21. ISBN: 978-3-942939-00-3

[25] Rohacs D, Farkas Cs, Ovari Gy, Rohacs J. Time and cost minimized integrated product and production process development for customized low volume advanced technology. In: Repüléstudományi Közlemények, XXIX; 2017. No. 3

[26] Nicols. Turbulence Models and Their Application to Complex Flows. 4.01 version. onlines guide. https://overflow.larc.nasa.gov/files/2014/06/Turbulence_Guide_v4.01.pdf (downloaded at 16 of July, 2017)

[27] Krasnov NF. Prikladnaya Aerodinamika (Practical Aerodynamics—in Russian). Moscow: Vysshaya Skola; 1975. 731 p

[28] Kimberlin RD. Flight Testing of Fixed Wing Aircraft. AIAA; 2003. 435 p

[29] Klein V, Morelli EA. Aircraft System Identification—Theory and Practice. AIAA Education Series; 2006. 499 p

[30] Central Aerohydrodynamic Institute. Photo gallery. Downloaded at 16 of July, 2017; http://tsagi.com/pressroom/photogallery/

[31] Martynov AK. Prikladnaya aerodinamika [Practical Aerodynamics – in Russian]. Moscow: Vysshaya Skola; 1972. 448 p

[32] Saltzman EJ, Ayers TG. Review of flight-to-wind-tunnel drag correlation. Journal of Aircraft. 1982;**10**:801-811

[33] Torenbeek E. Synthesis of Subsonic Airplane Design. Delft: Delft University Press; 1976. 598 p

[34] Obert E. Aerodynamic Design of Transport Aircraft. Delft: Delft University Press, IOS Press; 2009. 656 p

[35] Küchemann D. The Aerodynamic Design of Aircraft. Oxford, New York: Pergamon Press; 1978. 564 p

[36] Roskam J. Airplane Design Part VI: Preliminary Calculation of Aerodynamic Thrust and Power Characteristics. Sixth Printing. Lawrance, Kansas, US: Dar Cooperation; 2017. 584 p

[37] Sobester A, Forrester AIJ. Aircraft Aerodynamic Design: Geometry and Optimization. John Wiley and Sons; 2014. 262 p

[38] Abott IA, Doenhoff AE, Stivers LS Jr. Summary of Airfoil Data. NACA Report No. 824; 1945. 261 p. https://ntrs.nasa.gov/archive/nasa/casi.ntrs.nasa.gov/19930090976.pdf [visited at 12 July 2017]

[39] UIUC Airfoil Coordinates Database. UIUC Applied Aerodynamics Group, Department of Aerospace. http://m-selig.ae.illinois.edu/ads/coord_database.html [visited at 12 July 2017]

[40] Bryan GH. Stability in Aviation. Macmillan & Co.; 1911. 192 p

[41] Cowley WL, Glauert H. Effect of the lag of the Donwash on the longitudinal stability of an airplane and on the rotary derivative Mq. ARC R&M 718; 1921

[42] Горбатенко СА, Макашов ЭМ, Полушкин ЮФ, Шефтель ЛВ. Механика полета: (Общие сведения. Уравнения движения). Инженерный справочник, Машиностроение, Москва; 1969. 420 с

[43] Белоцерковский С, Скрипач Б. Аэродинамические производные летательного аппарата и крыла при дозвуковых скоростях, Наука, Москва; 1975. 424 с

[44] Thomas HHBM. Some thoughts on mathematical models for flight dynamics. Aeronautical Journal. 1984;May:169-179

[45] Etkin B. Dynamics of Atmospheric Flight. Mineola, New York: Dover Publications; 2000. 582 p

[46] McRuer D, Ashkenas I, Graham D. Aircraft Dynamics and Automatic Control. Princeton University Press; July 1990

[47] Polhamus EE. A Concept of the Vortex Lift of Sharp-Edge Delta Wings Based on Leading-Edge-Suction Analogy. Washington: NASA; 1966. p. 18

[48] Napolitano M. Aircraft Dynamics: From Modeling to Simulation. J. Wiley & Sons; 2011

[49] Tobak M. On the use of the indicial function concept in the analysis of unsteady motion of wings and wing-tail combinations. NACA Report 1188. 1954. 47 p

[50] Leishman JG. Validation of approximate indicial aerodynamic functions for two-dimensional subsonic flow. Journal of Aircraft. 1988;**25**(10):914-922. DOI: https://doi.org/10.2514/3.45680

[51] Goman MG, Stolyarov GI, Tyrtyshnikov SL, Usoltsev SP, Khrabrov AN. Mathematical description of aircraft longitudinal aerodynamic characteristics at high angles of attack accounting for dynamic effects of separated flow. TsAGI Preprint No. 9; 1990 (in Russian)

[52] Goman M, Khrabrov A. State-space representation of aerodynamic characteristics of an aircraft at high angles of attack. AIAA Paper 92–4651-CP; 1992

[53] Zhang M, Yao Y, Wang H. Aircraft Takeoff Taxiing Model Based on Lagrange Interpolation Algorithm in Theory, Methodology, Tools and Applications for Modeling and Simulation of Complex Systems, Part 2. In: Zhang L, Song X, Wu Y, editors. 16th Asia Simulation Conference and SCS Autumn Simulation Multi-Conference AsiaSim/SCS AutumnSim 2016; Beijing; Oct. 8–11, 2016 Proceedings; Singapore: Springer. 2016. pp. 100-108

[54] Popov AV, Botez RM, Labib M. Transition point detection from the surface pressure distribution for controller design. Journal of Aircraft. 2008;**45**(1):23-28

[55] Dinu AD, Botez RM, Cotoi I. Chebyshev polynomials for unsteady aerodynamic calculations in aeroservoelasticity. Journal of Aircraft. 2006;**43**(1):165-171

[56] Wagner H. Über die Entstehung des dynamischen Auftriebes von Tragflügeln. Zeitschrift für Angewandte Mathematic und Mechanik. 1925;**5**(1):17-35

[57] Theodorsen T. General theory of aerodynamic instability and the mechanism of flutter. Technical Report, Report 496. National Advisory Committee for Aeronautics; 1935

[58] Brunton SL, Rowley CW. Empirical state-space representations for Theodorsen's lift model. Journal of Fluids and Structures. April 2013:174-186

[59] Kurniawan R. Numerical Study of Flutter of a Two-Dimensional Aeroelastic System. Hindawi Publishing Corporation ISRN Mechanical Engineering Volume. 2013. 4 pp. [Article ID 127123]. DOI: http://dx.doi.org/10.1155/2013/127123

[60] Herman JF, Washington ES. Wind Tunnel Investigation of the Aerodynamic Hysteresis Phenomenon on the F-4 Aircraft and Its Effect on Aircraft Motion. US Air Force Report, AEDC-TR-80-10. Aernold Engineering Development Centre. 1980. 95 p

[61] Tobak M, Chapman GT. Nonlinear problems in flight dynamics involving aerodynamic bifurcations. NASA TM 86706; 1985

[62] Yang Z, Igarashi H, Martin M, Hu H. An experimental investigation on aerodynamic hysteresis of a low-Reynolds number airfoil. In: 46th AIAA Aerospace Sciences Meeting and Exhibit; Jan 7–10 2008; Reno, Nevada. AIAA-2008-0315, 11 p

[63] Khrabrov AN, Kolinko KA, Vinogradov YA, Zhuk AN, Grishin II, Ignatyev DI. Experimental investigation and mathematical simulation of unsteady aerodynamic characteristics of a transonic cruiser model at small velocities in a wide range of angles of attack. Visualization of Mechanical Processes: An International Online Journal. 2011;**1**(2). DOI: 10.1615/VisMechProc.v1.i2.40

[64] Ericsson LE. Dynamic stall at high frequency and large amplitude. Journal of Aircraft. 1980;**8**:136-142

[65] Wang Z, Li J. Lan CE, Brandon JM. Estimation of unsteady aerodynamic models from flight test data. AIAA Atmospheric Flight Mechanics Conference and Exhibit, Guidance, Navigation, and Control and Co-located Conferences; Montreal. 2001. https://doi.org/10.2514/6.2001-4017

[66] Harper PW, Flanigan RE. The effect of rate of change of angle of attack on the maximum lift of a small model. Technical Note. NACA TN-2061. 1950. 21 p

[67] Favier D, Agnes A, Barbi C, Maresca C. Combined translation/pitch motion: A new airfoil dynamic stall simulation. Journal of Aircraft. September, 1988:805-813

[68] F/A-18 Stability and Control Data Report. Volume I: Low Angle of Attack. Report # MDC A7247. Issue date 31 August 1981. Revision date 15 November 1982. Revision letter B, McDonell Aircraft Company 3

[69] F/A-18 Stability and Control Data Report. Volume II: High Angle of Attack. Report # MDC A 7247. Issue date 31 August 1981. McDonell Aircraft Company

[70] Katz J, Maskew B. Unsteady low-speed aerodynamic model for complete aircraft configuration. Journal of Aircraft. 1988;April:302-310

[71] Barth TJ, Planeaux P. High angle of attack dynamic behaviour of a model of high performance fighter aircraft. AIAA Paper 88-4368. 1988

[72] Carroll JV, Mehra SB. Bifurcation analysis of nonlinear aircraft dynamics. Journal of Guidance. 1982;**5**:529-536

[73] Mehra SB, Carroll JV. Global stability and control analysis of aircraft at high angles—of—attack. Annual Technical Report, N00014-76-C-0780; Aug. 1979. 356 p. file:///C:/Users/joe/Downloads/ADA084938.pdf, [downloaded at 12 May 2017]

[74] Gao H, He ZD, Zhou ZQ. The study of global stability and sensitivity analysis at high performance aircraft at high angles - of – attack. In: Congress of the International Council of Aeronautical Sciences (ICAS/AIAA); 1988; Jerusalem. 1988. pp. 1356-1363

[75] Jahnke CC, Culick FEC. Application of bifurcation theory to the high-angle-of-attack dynamics of the F-14. Journal of Aircraft. 1994;**31**(1):26-33

[76] Guicheteau P. Bifurcation theory in flight dynamics an application to a real combat aircraft. In: Proceedings of 17th ICAS (International Council of Aeronautical Science) Congress, ICAS-90-5.10.4; Stockholm, Sweden. 1990. pp. 1990-1998

[77] Moes TR, Noffz GK, Iliff KW. Results from F-18B stability and control parameter estimation flight tests at high dynamic pressures. NASA/TP-2000-209033. NASA; 143 p

[78] Cao J, Garret F Jr, Hoffman E, Stalford H. Analytical aerodynamic model of a high alpha research vehicle wind-tunnel model. NASA CR-187469. 1990

[79] Linse DJ, Stengel RF. Identification of aerodynamic coefficients using computational neural networks. Journal of Guidance, Control, and Dynamics (ISSN 0731–5090). 1993;**16**(6):1018-1025

[80] Rajkumar T, Bardina J. Prediction of aerodynamic coefficients using neural network for sparse data. In: Proc. of FLAIRS (Florida Artificial Intelligence Research Society Conference); Pensacola, Florida, US. 2002. pp. 242-246

[81] Secco NR, de Mattos BS. Artificial neural networks to predict aerodynamic coefficients of transport airplanes. Aircraft Engineering and Aerospace Technology. 2017;**89**(2):211-230. DOI: https://doi.org/10.1108/AEAT-05-2014-0069

[82] Ignatyev DI, Khrabov AN. Application of neural networks in simulation of dynamic effects of canard aircraft aerodynamics. TsAGI Science Journal. 2011;**42**:817-828

[83] Rajkumar T, Aragon C, Bardina J, Britten R. Prediction of aerodynamic coefficients for wind tunnel data using a genetic algorithm optimized neural network. In: Zanasi A,

Brebbia CA, Ebecken NFFE, Melli P, editors. Third International Conference on Data Mining, 2002, Bologna, Italy in "Management Information Systems". pp. 473-487

[84] de Visser CC, Mulder JA, Chu QP. Global aerodynamic modeling with multivariate splines, AIAA-2008-7500. In: AIAA Modeling and Simulation Technologies Conference and Exhibit; Honolulu, HI; August 2008

[85] Kouba G, Botez RM, Boely N. Fuzzy logic method use in F/A-18 aircraft model identification. Journal of Aircraft. 2010;**47**(1):10-17. DOI: https://doi.org/10.2514/1.40714

[86] Wang Z, Lan C, Brandon J. Fuzzy logic modeling of nonlinear unsteady aerodynamics. In: 23rd Atmospheric Flight Mechanics Conference, Guidance, Navigation, and Control and Co-located Conferences, AIAA-98-4351; Boston. 1998

[87] Mohammadi SJ, Sabzeparvar M, Karrari M. Aircraft stability and control model using wavelet transforms. Institution of Mechanical Engineers, Part G: Journal of Aerospace Engineering. 2010;**224**:1107-1118

[88] Mader CA, Joaquim R, Martins RA. Computing stability derivatives and their gradients for aerodynamic shape optimization. AIAA Journal. 2014;**52**(11):2533-2546

[89] Brandon JM, Morelli EA. Real-time onboard global nonlinear aerodynamic modeling from flight data. Journal of Aircraft. September;**53**(5):1261–1297

[90] Mavris DN, Kirby MR. Technology identification, evaluation and selection for commercial transport aircraft. Presented at 58th Annual Conference of Society of Allied Weight Engineers, Inc.; San Jose, CA; 24–26 May 1999; Georgia Institute of Technology. SAWE Paper No. 99-2456

[91] Kirby MR. A methodology for technology identification, evaluation and selection in conceptual and preliminary aircraft design [PhD thesis]. Georgia Institute of Technology; 2001

[92] Veress A, Bicsak G. New adaption of actuator disc method for aircraft propeller CFD analyses. Acta Polytechnica Hungarica [Journal of Applied Sciences Hungary]. 2017

[93] Veress Á, Bicsák G, Rohács D. Pressure loss and flow uniformity analysis of baseline and redesigned engine inlet duct for a small turboprop aircraft. Czech Aerospace Proceedings. 2016;**1**:3-9

[94] Rohacs J, Veress A, Jankovics I, Volescsuk A, Farkas Cs. Goal oriented aerodynamic design of a new acrobatic aircraft, research and education in aircraft design. In: READ 2010 International Conference; Warsaw, Poland; June 28-30, 2010; Proceeding CD. 10 p. ISSN 1425-2104

[95] Jankovics IR, Rohacs D, Rohacs J. Motion simulation model of a special acrobatic aircraft. In: Proceedings of the 12th MINI Conference on Vehicle System Dynamics, Identification and Anomalies; Budapest University of Technology and Economics; 2012. pp. 393-401 ISBN: 978-963-313-058-2

[96] Hargitai LC, Rohács D. Motion simulation of inland vessels. Brodogradnja. 2017;**67**

[97] Rohacs D, Rohacs J. Magnetic levitation assisted aircraft take-off and landing (feasibility study—GABRIEL concept). Progress in Aerospace Sciences. 2016;**85**:33-50. DOI: 10.1016/j.paerosci.2016.06.001

[98] Rohacs D, Voskuijl M, Siepenkotter N. Evaluation of landing characteristics achieved by simulations and flight tests on a small-scaled model related to magnetically levitated advanced take-off and landing operations. Proceedings of the 29th Congress of the International Council of the Aeronautical Sciences (ICAS); St. Petersburg, Russia; 07/09/2014–12/09/2014. Paper Rohacs_et al. 9 p

[99] Rohacs D, Voskuijl M, Pool D, Siepenkötter N, Sibilski K. Aircraft magnetic levitated advanced take-off and landing concept validation. Periodica Polytechnica. 2018

[100] Rohács J, Thomasson P, Mosekilde E, Gránásy P. Effects of non-linearities on aircraft poststall motion. In: Nonlinear Problems in Aviation and Aerospace; INCPAA Proceedings; 1996 May, 9–11; Daytona Beach, Florida, USA. 1996. pp. 601–609

[101] Rohács J, Gránásy P. In: Sivasundaram S, editor. Effects of Non-Linearities in Aerodynamic Coefficient on Aircraft Longitudinal Motion, Non-Linear Problems in Aviation and Aerospace. New York: Gordon and Breach; 2000. pp. 281-296

[102] Rohacs J, Bathory ZS. Analysis of approximation of aircraft stochastic motion by markov models. In: ICAS Congress; Yokohama, Japan; CD-ROM, 2004, ICAS. 2004.10.2.1–4.10.2.10. http://www.icas.org/ICAS_ARCHIVE/ICAS2004/PAPERS/324.PDF

[103] Rohács J. Unconventional flight analysis. In: "21st Congress of the International Council of Aeronautical Sciences"; 13–18 September 1998; Melbourne, Victoria, Australia; ICAS Technical Proceedings on CD-ROM, Sept., 1998. A98-31457, Paper 98-1,4,3

[104] Rohács J. Bifurcation analysis of aircraft poststall motion. In: Proceedings of the 7th Mini Conference on Vehicle System Dynamics, Identification and Anomalies, Budapest 2000; Budapest: Department of Railway Vehicles, BUTE. 2001. pp. 53-76

IntechOpen